**NASA
Technical
Paper
3255**

February 1993

Manual Flying of Curved Precision Approaches to Landing With Electromechanical Instrumentation

A Piloted Simulation Study

Charles E. Knox

NASA
Technical
Paper
3255

1993

Manual Flying of Curved Precision Approaches to Landing With Electromechanical Instrumentation

A Piloted Simulation Study

Charles E. Knox
Langley Research Center
Hampton, Virginia

Summary

A piloted simulation study was conducted to examine electromechanical flight instrumentation for use on curved precision approaches to a landing. Horizontal and vertical path tracking situation information and flight guidance during manually controlled flight in the microwave landing system (MLS) signal environment were examined during this study. These approach paths were contained within the signal coverage area of the time-referenced scanning beam MLS as specified by the International Civil Aviation Organization. The data from these tests indicated that flight director guidance is required for the manually controlled flight of a jet transport airplane on curved approach paths. Acceptable path tracking performance was attained with each of three situation information algorithms tested. However, pilot comments indicated that during turns the use of lateral tracking situation information based on capturing the next straight path segment may not be acceptable, since full-scale lateral deviation indications normally resulted during turns. Pilot comments indicated that two of the three curved approach paths tested could be used in normal airline operations. They felt that the third approach path would be acceptable if the decision height altitude and the visibility minimums were greater. Approach paths with both multiple sequential turns and short final path segments were evaluated.

Introduction

The National Airspace System Plan of the Federal Aviation Administration currently calls for the present instrument landing system (ILS) to be replaced by the microwave landing system (MLS). The MLS offers a number of technical and operational capabilities over the ILS, one of which is the expanded area of proportional signal coverage. (The MLS provides up to $\pm 60°$ azimuth and $20°$ elevation compared with the ILS, which provides $\pm 3°$ to $\pm 6°$ azimuth and approximately $\pm 0.7°$ angular elevation about a nominal $3°$ glide slope.) The expanded signal coverage has the potential to support multiple, curved approach paths that could be used for noise abatement, obstacle clearance, vortex avoidance, and instrument approach capability to runways or landing pads not directly associated with an MLS facility (ref. 1). Other simulation studies have indicated a reduction of controller/pilot communications workload and potentially significant increases in airport capacity (ref. 2).

However, many operational considerations of precision approaches (an approach with an electronically generated glide slope) with multiple straight and curved flight path segments must be addressed before realizing benefits. Some of these operational considerations include the requirements for flight guidance and situation information, the geometrical definition of the approach path, and pilot acceptance of curved precision approaches.

In today's flight environment, the final segment of a precision approach is flown on a straight-in path before reaching an altitude where the landing must be completed by visual reference to the runway environment. There is no requirement to use flight director command guidance to fly a straight-in precision approach. However, in the MLS signal environment, a precision approach could contain multiple turns and may be too difficult to be flown without flight director command guidance. This report will examine the need for flight director guidance to fly very complex curved approach paths.

In addition to the issue of flight director guidance requirements, there has been much discussion about the required type of situation information (lateral and vertical path tracking errors, etc.). There are also questions as to how the electromechanical flight instrumentation should be driven.

To address these issues, three situation information algorithms for driving conventional electromechanical flight instrumentation for manually controlled flight along curved approach paths were evaluated. The first algorithm, called the "segmented algorithm," provided lateral deviation information during turns emulating a typical instrument landing system localizer capture. The second and third algorithms provided continuous path deviations relative to a circular path. The second algorithm utilized turn radii as specified in the approach procedure. The third algorithm computed a radius for the turn based on the ground speed of the airplane just prior to beginning the turn.

The approach paths used during these tests had multiple turns, with turn radii between 7500 ft and 20 000 ft, and vertical transitions (changes in programmed flight path angle) between $1.7°$ and $4.5°$. The final straight-in leg segments for the approaches varied between ½ mile and 3 miles.

Path tracking accuracy and pilot acceptance and comments were used for the evaluation of the guidance and situation information tested. This report will summarize the results of the study.

Symbols and Abbreviations

ADI	attitude director indicator
AGL	above ground level

DME	distance measuring equipment
FD	flight director
HSI	horizontal situation indicator
HOOK	HOOK instrument approach procedure
ILS	instrument landing system
MLS	microwave landing system
OFFSET	OFFSET approach procedure
RIVER	RIVER approach procedure
RMI	radio magnetic indicator
rms	root mean square
SLINE	straight line (ILS replica) approach
γ	flight path angle

Simulator Description

This study was conducted in the NASA Langley Visual/Motion Simulator (VMS). The VMS is a six-degree-of-freedom, motion-base simulator capable of presenting realistic acceleration and attitude cues to the pilot. A general-purpose, scientific mainframe computer with a nonlinear, digital representation of a McDonnell Douglas DC-9 airplane provided inputs to drive the VMS simulator. Audio cues for engine thrust and aerodynamic buffet were also provided. The simulator had a generic cockpit with conventional flight controls and instrumentation. Flight controls included a column and control wheel, rudder pedals, throttle, speed brake, and flap controls located on a center console. Flight instrumentation included conventional flight and navigation instruments and engine instrumentation. A forward-looking out-the-window visual scene of the runway environment was provided to each pilot. The VMS facility is described in more detail in reference 3.

Flight Instrumentation Description

Figure 1 shows the arrangement of the flight instrument panel used during the simulation tests. The flight instrumentation was arranged in a standard "T" format and, with several exceptions, functioned in a conventional manner. The top of the "T," from left to right, consisted of a combined airspeed/Mach number indicator, an attitude director indicator (ADI), and a barometric counter-drum-pointer altimeter.

Figure 2 shows a larger picture of the ADI. The ADI contained a dual-cue flight director programmed to give commands to the pilot for tracking the vertical and lateral paths that lead to the runway. On the left-hand side of the ADI was a fast/slow bug that indicated airspeed deviations up to ±20 knots from a reference speed set by the pilot on the airspeed/Mach number indicator. The ADI also contained a lateral-path-deviation indicator needle with full-scale indications of ±1500 ft and a vertical-path-deviation indicator needle with full-scale indications of ±250 ft.

The vertical portion of the standard "T" was formed by the horizontal situation indicator (HSI) centered below the ADI. The basic information displayed on this HSI, shown in figure 3, was similar to that shown on a conventional HSI. A rotating compass rose indicated the magnetic heading of the airplane, and a course deviation indicator showed the direction and lateral displacement (±1500-ft full-scale deflection) of the airplane relative to a desired track. During these tests, the situation information algorithm computed the desired track angle and automatically set the course deviation indicator instead of requiring the pilot to set it manually as with a conventional HSI. The track angle of the desired course was also displayed digitally in the upper right-hand corner of the HSI.

The HSI used during these tests had a bearing pointer arrow that rotated about the compass rose. During these tests, this arrow was used as an advance-track-angle arrow. It was driven by the situation information algorithm to indicate the desired course direction at the end of turn segments. Five seconds before the airplane was to begin a turn, the arrow would be driven to the desired track angle at the end of the turn, thus giving the pilot a pictorial view of where he would be rolling out of the turn. The advance-track-angle arrow would remain in that position on the compass rose until the airplane reached the beginning of the next turn.

The remaining situation information features on the HSI included a vertical-path-deviation indicator with full-scale deviations of ±250 ft, a heading reference on the compass rose that could be manually set by the pilot, and a digital readout in the upper left-hand corner of the HSI used to indicate the active waypoint number upon which the situation information algorithm computations were based.

The remaining basic flight instrumentation on the instrument panel included a vertical speed indicator and a turn and bank indicator located below the altimeter. These instruments operated in a conventional manner. A distance measuring equipment (DME) indicator and a radio magnetic indicator (RMI) were located below the airspeed/Mach number indicator. This DME indicator displayed the slant-range distance between the airplane and

the DME ground facility collocated with the MLS azimuth antenna. The RMI displayed the relative bearing of the MLS ground system azimuth antenna from the airplane.

A second DME indicator was located below the HSI. The distance shown on this instrument was the "along track" distance, which was computed by the situation information algorithm as the distance along the programmed path between the airplane and the glide path intercept point on the runway.

Two annunciator lights were used to indicate changes in direction and flight path angle of the programmed path. A light centered over the ADI was illuminated 5 sec before the airplane was to begin a turn and was extinguished at the end of the turn. When no turn was programmed, the light was illuminated 5 sec before the airplane crossed a waypoint and was extinguished 10 sec after the waypoint was crossed. During all other straight path segments, this light was off.

The second annunciator light was located to the right side of the ADI adjacent to the vertical-path-deviation indicator. This light would blink for 5 sec when the vertical flight path angle of the programmed path changed more than 1°. The light was also continuously illuminated whenever the programmed path required a descent.

Situation Information Algorithms

The situation information algorithms used in the area navigation system for this study computed the path definition and deviations with vector algebra within an Earth-centered coordinate system (ref. 4). Lateral paths are computed as great circle segments between successive waypoints. Turns at waypoints are computed as circular transitions between the inbound path and the outbound path at each waypoint. Lateral deviation is computed with vector algebra as the distance between the lateral path and the airplane along a line perpendicular to the lateral path.

Vertical paths are defined as linear altitude changes between two reference points. These reference points may be defined at the actual waypoints, at the center of the turn arc at a waypoint, or at the beginning or end of the turn arc at a waypoint. Vertical deviation is computed in a simple equation as the difference between the altitude of the airplane and the desired altitude along the leg segment between the two reference points. The desired altitude along the leg segment is proportional to the distance traveled along the leg segment divided by the total leg segment length and the altitudes assigned to the two waypoints.

During these tests, three turn algorithms were evaluated to compute path definition and path tracking deviations. These algorithms were called "segmented"; "circular, fixed radius"; and "circular, computed radius" algorithms. Each algorithm used identical computations for determining lateral and vertical deviations for the straight line segments between two waypoints. However, during turns, each algorithm differed significantly in computation and situation information presentation.

Figures 4 through 6 illustrate the differences between the three algorithms during a turn. The turn used as an example in each of these figures was a 90° turn to the right. Prior to the start of the turn, the inbound path segment to the waypoint (named WPT04 in figs. 4 through 6) was at a constant altitude of 2300 ft. The outbound segment from the waypoint had a constant flight path angle descent to cross the next waypoint at an altitude of 1000 ft. The format in figures 4 through 6 shows a vertical and an oblique profile view. In the oblique view, the observer is located inside the turn close to its center. The beginning of the turn is on the left-hand side of the figure, and the end of the turn is on the right-hand side. The vertical profile view shows where the vertical path transitions occurred and has been drawn so that the turn entry and exit points and the waypoint locations coincide vertically with those in the oblique view. In each of these figures, the airplane is displaced the same distance laterally inside, and vertically below, the desired path. A drawing of the ADI and HSI with the lateral- and vertical-path-deviation indicators shows the indications displayed to the pilot for each of the three algorithms.

Segmented Algorithm

The segmented algorithm was designed to provide lateral path deviations and course guidance that would emulate the display indications seen by the pilot during a routine capture of the final straight segment of the ILS localizer. The vertical path deviations and course guidance were designed to be continuous and had an interim, constant flight path angle segment to reduce the amount of each vertical path change.

The path geometry definition and flight instrument indications for the segmented algorithm are illustrated in figure 4. The vertical profile view shows that the transition from level flight on the inbound path segment to the descent on the outbound segment of the programmed path was a two-step process begun at the start of the turn and completed at the end of the turn. The flight path angles of the inbound and outbound leg segments were computed

as the inverse tangent of the difference in assigned altitude of consecutive waypoints divided by the direct horizontal distance between the waypoints. In this example, the inbound leg segment was at level flight, or flight path angle of $0°$, and the outbound leg at a descent angle of $-2.71°$.

During the turn segment connecting the inbound and outbound legs, a constant flight path angle equal to the inverse tangent of the difference of the programmed altitudes at the beginning and the end of the turn divided by the turn arc length is computed. In this example, the flight path angle during the turn is $-1.73°$.

The flight path angle changes at the beginning and the end of the turn were anticipated by the flight director commands so that the crossing would be smooth. This was accomplished by changing the desired flight path angle to be flown in the flight director from the angle of the leg segment being flown to the angle of the next leg at a rate of $0.5°/\text{sec}$. This change would be started such that the desired flight path angle of the next leg segment would occur just as the airplane started the next segment.

Lateral steering commands provided by the flight director during the turns were based on tracking circular paths with turn radii defined in the approach procedure. At the beginning of each turn, the advance-track-angle arrow and the course deviation indicator on the HSI were rotated rapidly (in less than 1 sec) to the track angle of the outbound path segment, and the lateral path deviation displayed to the pilot was computed relative to the outbound segment. It should be noted that full-scale deflections could be observed at the beginning of each turn, depending on the geometry of the turn and the scaling of the lateral-path-deviation indicator.

Circular, Fixed Radius Algorithm

The circular, fixed radius algorithm was designed to provide continuous lateral path tracking while on circular path segments with turn radii defined in the approach procedure. Vertical path deviations and course guidance were designed to be continuous, with a single flight path angle change in the middle of the turn arc to reduce charting complexities and pilot task load.

The path geometry definition and flight instrument indications for the circular, fixed radius algorithm are illustrated in figure 5. The vertical profile view shows that the vertical transition from the inbound path segment to the outbound segment occurred when the airplane passed the midpoint of the turn arc. Flight path angle changes at the midpoint

of the turn arc were anticipated by the vertical flight director command in the same manner as described in the segmented algorithm section to achieve smooth commands.

It should also be noted that the vertical flight path angle of the outbound segment was $-3.1°$ for this algorithm and $-2.71°$ for the segmented algorithm. This difference is due to the way the longitudinal distance between waypoints was defined for each algorithm. The segmented algorithm used the straight line horizontal distance between waypoints to compute the flight path angle. The circular, fixed radius algorithm used the along track distance between the midpoint of the turn arc of the waypoint to the midpoint of the turn arc of the next waypoint, which is slightly shorter. This shorter path resulted in a slightly steeper descent path.

Lateral steering commands provided by the flight director during the turns were based on tracking the circular-arc path defined by the approach procedure, the same as with the segmented algorithm. However, the course deviation indicator, the lateral deviation, and the advance-track-angle arrow on the HSI were driven differently. The course deviation indicator was driven around the turn so that its direction was always tangent to the point to which the airplane had progressed on the path. The lateral deviation displayed to the pilot was computed relative to the tangent point on the circular-arc path.

The advance-track-angle arrow on the HSI was slewed rapidly, as with the segmented guidance, to the track angle of the outbound leg segment. The advance-track-angle arrow was slewed just prior to entering the turn and served as a point of reference for the turn to be completed.

Circular, Computed Radius Algorithm

The circular, computed radius algorithm was designed to provide continuous circular path situation information and guidance and to command an initial bank angle of $15°$ at the beginning of each turn. Using the same initial bank angle at the beginning of each turn would provide operational consistency for the pilot during the approach. The vertical path deviations and course guidance were the same as discussed in the segmented algorithm description.

The path geometry definition and flight instrument indications for the circular, computed radius algorithm are illustrated in figure 6. The turn radius used for this algorithm was different than for the two previous algorithms. While the previous algorithms used a fixed radius defined in the approach procedure, this algorithm used a radius computed

just prior to the beginning of each turn. The radius was computed for each turn based on a 15° initial bank angle and the ground speed of the airplane. Once the turn was started, the radius was kept constant and the pilot had to vary the airplane bank angle to compensate for changing ground speed and wind conditions to fly on the circular path.

The vertical situation information and guidance were the same as described in the segmented algorithm section. However, it should be noted that while the flight path angle of the turn segment cannot exceed the descent or ascent values of inbound or outbound leg segments, it will vary depending upon the magnitude of the turn radius.

Transition From Linear Path Deviations to MLS Angular Deviations

Each algorithm computed path deviations and flight director steering commands based on a position estimate derived with MLS azimuth angle signals, MLS DME signals, and altitude from the barometric altimeter. While in this position estimate mode, path deviations were computed and displayed as linear distances with constant, full-scale sensitivities on the lateral- and vertical-path-deviation indicators of ±1500 ft and ±250 ft, respectively. However, once the airplane had completed the final turn to the straight-in path segment to the runway, computations for path deviations and steering commands were based on "raw" MLS azimuth and elevation angular signals. This resulted in the deviation indicators being displayed with constant angular sensitivities similar to those used with a conventional ILS receiver. The full-scale deviation indicator sensitivity, when the MLS angular signals were displayed directly, was ±3° laterally and ±0.7° vertically.

To preclude the possibility of large jumps in the lateral and vertical deviation indications and the flight director commands during the transition from linear to angular situation information, it was necessary to match the maximum full-scale deviation of the linear-path-deviation indications to that obtained with the angular indications. This was accomplished by reducing the full-scale lateral indication from ±1500 ft to an amount equivalent to a ±3° angle when the airplane was a distance along the programmed flight path of 28 622 ft from the azimuth antenna (tan 3° multiplied by the along track distance between the airplane and the MLS azimuth antenna). Full-scale vertical deviations were reduced in a similar manner, from ±250 ft to ±0.7°, when the airplane was a distance along the programmed path of 20 462 ft from the elevation antenna.

Approach Flight Paths and Instrument Procedures

Four approach paths were used during these evaluation tests. One approach was designed to emulate a typical ILS approach and was used as a baseline for comparison of tracking accuracy and the pilot's perceived workload assessment obtained on the more complex curved paths. The other three paths were curved paths designed to determine situation information requirements due to the effects of multiple turns and/or descent segments, large and small turn radii, and short straight-in final approach segments.

The instrument approach procedures used by the pilots to fly the approach paths are shown in figures 7 through 13. These procedures were charted in a format similar to the standard instrument approach procedures published by the U.S. Government. Each procedure was charted to runway 22 at the Wallops Flight Facility at Wallops Island, Virginia.

The plan view of the three MLS curved paths was charted in two slightly different formats. In one format (figs. 8, 10, and 12), the turn radii were not specified. In the other format (figs. 9, 11, and 13), a specific radius and curved path were defined for each turn. Both charting procedures were required, since one of the situation information algorithms computed the turn radius based on the ground speed of the airplane and the other two used the radii specified in the procedure.

SLINE Approach Procedure

The SLINE (straight line) approach procedure is shown in figure 7. Although the situation information used for this approach was computed with the segmented algorithm used for the curved path approaches, guidance for the pilot replicated a typical ILS approach. The resulting tracking data and pilot comments were used as conventional ILS baseline data to compare with the curved path data.

OFFSET Approach Procedure

The OFFSET approach procedure is shown in figures 8 and 9. This approach began with a level flight segment that was offset and parallel to the runway centerline. A right 90° turn followed immediately by a left 90° turn, without a straight segment between turns, was programmed to bring the airplane to the final approach segment. Back-to-back successive turns were programmed to determine if there were any adverse effects from not having an intermediate straight segment to allow for airplane stabilization. A descent was begun at the first turn. At the

5

end of the final turn there was a 3-mile-long straight-in final approach segment. This was the longest final approach segment for the curved paths in this test.

HOOK Approach Procedure

The HOOK approach procedure is shown in figures 10 and 11. This approach was designed to determine the effects of vertical path transitions during a turn (level flight to a descent and a descent to level flight). Turn radii varied from 20 000 ft at the first turn to 7500 ft at the final turn. This approach also had two, opposite direction, 90° turns, but with a short straight segment between them. At the end of the final turn there was a 2-mile-long straight-in final approach segment.

RIVER Approach Procedure

The RIVER approach procedure to runway 22 at Wallops Flight Facility is shown in figures 12 and 13. The approach path geometry of this procedure has the same path as the River Visual Runway 18 instrument approach procedure into the Washington National Airport (ref. 5). This flight path was chosen because of the large number of turns that occur in a short distance. The straight-in final approach segment after the last turn on this path was ½ mile long and was the shortest final approach segment tested.

Simulation Tests

The simulator tests were designed to provide data for use in formulating situation information and command guidance requirements when using electro-mechanical flight instrumentation for flight along complex curved paths. This was accomplished through the evaluation of three turn algorithms. Tracking performance data, control activity, pilot eye scan patterns, and pilot comments were used for the evaluation. No attempt was made during these tests to investigate the system interface requirements necessary for the pilot to program or select the approach path.

Test Conditions

Table I shows the test matrix and number of test runs completed by each of the pilots. Each of the three turn algorithms (segmented; circular, fixed radius; and circular, computed radius) were evaluated *with* flight director command guidance for each of the curved paths (HOOK, OFFSET, and RIVER approaches). In addition, the segmented algorithm was evaluated *without* flight director command guidance for each of the curved paths. The straight-in path (SLINE approach) was flown with only the segmented algorithm, both with and without the use of

flight director command guidance. The test runs using the SLINE approach were used as baseline data, since this approach replicated a standard ILS approach procedure. The SLINE approach procedure was flown with the use of flight director guidance twice at the beginning and twice at the end of each of the three test days.

Table I. Test Matrix and Number of Approaches Completed by Each Test Subject

	Flight director on						Flight director off	
	Circular, computed radius algorithm		Circular, fixed radius algorithm		Segmented algorithm		Segmented algorithm	
Approach procedure	Wind	No wind	Wind	No wind	Wind	No wind	Wind	No wind
HOOK	2	2	2	2	2	2	2	1
OFFSET	2	2	2	2	2	2	2	1
RIVER	2	2	2	2	2	2	2	1
SLINE					6	6	1	1

Two wind models were used during these tests. Each test subject flew each test condition once with wind model 1 and once with model 2. The wind models were designed to vary linearly in both direction and magnitude as a function of altitude. The speed of the wind in both models was 15 knots at the surface and increased at a rate of 5 knots/1000 ft of increase in altitude. The direction of the wind at the surface in model 1 was 272° (60° crosswind from the right) and in model 2 was 152° (60° crosswind from the left). The wind direction in model 1 rotated 10° clockwise in direction for each 1000-ft increase in altitude. Wind model 2 rotated counterclockwise 10° for each 1000-ft increase in altitude.

Turbulence was modeled according to the Dryden spectra described in reference 6. The turbulence was generated with a mean of zero and a standard deviation of 4 ft/sec. The test subjects described this turbulence as light to moderate.

Test Subjects

Six subject pilots were used during these tests. Four of the pilots were employed as management or training pilots by an international air carrier. Each of these pilots actively flew commercial operations for their companies. The other subject pilots were rated in transport airplanes and employed by NASA.

Test Procedures

The test period for each pilot lasted 3 consecutive days. The first ½ day of this period was spent on familiarization. The pilot was briefed on the purpose of the test, how the situation and guidance information was computed and displayed on the flight instruments, the approach procedures and charts, and the aircraft speed and flap limitations.

During the familiarization period, each test subject flew a minimum of nine approaches using each of the three situation information algorithms (all with flight director commands) on each of the three curved paths. Turbulence and winds were not introduced at this time so that the subject pilot could devote more of his attention to the guidance and situation information. The practice runs were stopped and then continued if the pilot had any questions about the simulation.

Test runs for recorded data began in the afternoon of the first day. Each approach was begun with the airplane established on course at the first waypoint. The pilot was told that he should complete the approach and land if he could, but he was to execute a missed approach if he did not feel that the airplane was stabilized or in a position from which a landing could be made.

The test conductor functioned as copilot during the test runs, performing normal copilot duties such as calling checklists, selecting flaps and gear upon the pilot's command, and giving the pilot verbal "call outs" when the airplane was 1000 ft AGL, 500 ft AGL, 300 ft AGL, and when the 200-ft AGL decision height was reached. He also called attention to abnormal flight conditions such as excessive vertical speeds, high and low airspeeds, and excessive path tracking errors. After each approach, the test conductor would record comments made by the pilot.

Recorded Data

The following data were recorded during each approach: (1) digital data that described the state of the airplane, path tracking parameters, and flight control surface activity at a 5.3-Hz sample rate (once every sixth computational frame); (2) oculometer eye scan of the instrument panel at a 32-Hz sample rate—a complete description of the oculometer system and specific parameters recorded may be found in reference 7; (3) video recording of the instrument panel with an eye scan dot superimposed, indicating where the pilot was looking; and (4) pilot comments. No data were recorded during the familiarization period.

Method of Analysis

The recorded data were grouped into 10 sets, listed in table II, for comparison purposes from approximately 360 test runs. Various comparisons of these data sets were made to determine performance and workload differences between (1) flights with and without the use of flight director guidance, (2) flights on curved paths and straight-in (typical ILS approach) paths, and (3) flights on curved paths using the three situation information algorithms tested. The parameters used for comparisons included tracking performance, flight control activity, pilot eye scan, and pilot comments.

Table II. Data Sets Extracted From the Total Performance Data Base

Data set number	Paths	Situation information algorithms	Flight director
1	All curved	All	On
2	All curved	Segmented	Off
3	Straight in	Segmented	On
4	Straight in	Segmented	Off
5	All curved	Segmented	On
6	All curved	Fixed radius	On
7	All curved	Computed radius	On
8	RIVER	All	On
9	HOOK	All	On
10	OFFSET	All	On

Path tracking performance was evaluated using (1) lateral and vertical path tracking errors both for the entire path and at the 200-ft AGL decision height point (0.46 n.mi. from the runway threshold), (2) track angle errors for the entire path, (3) the vertical speed of the airplane at the decision height point, and (4) the distance from the approach end of the runway to where the airplane touched down. The tracking performance data for the entire path for each data set included the average and the standard deviation of the rms values of the tracking errors. These performance data were computed by first calculating the rms value of the lateral and vertical tracking errors for the entire path length for each test run. Then, with the rms values of the tracking errors for each test run, the average and standard deviation of each of these rms tracking errors were calculated for each data set. This same procedure was used to compute the track angle errors for each data set.

The rms value of the lateral and vertical path tracking errors and the vertical speed of the airplane

when the decision height point was crossed were computed from the lateral and vertical tracking errors attained when that point was crossed on each test run. The significance of the decision height on a precision approach is that it is the point at which the pilot must decide to land the airplane or to start proceeding with a missed approach procedure. The magnitudes of the lateral and vertical path tracking errors at the decision height point are very significant factors in the success of the landing, since only very limited maneuvering of the airplane can occur until the desired touchdown point on the runway is crossed. This is particularly true for airplanes with high approach speeds.

An indication of physical workload was identified through column and wheel input and reversal rates. Both wheel and column input and reversal rates (both having units of control inputs per second) were defined as the wheel or column being moved more than ½° during each data recording iteration (5.3-Hz sample rate). The wheel and column input reversal rates indicated the number of changes in the direction of the control inputs (i.e., push to pull on the column and left to right aileron input on the wheel). The average wheel and column input and reversal rates were computed for each test run. Then the mean and standard deviation of these rates were computed for each data set.

The pilot's eye scan was used to give additional understanding of his workload. The parameters used to analyze the pilot's eye scan were the average dwell time on each flight instrument, the percentage of average dwell time, and the percentage of transitions between particular flight instruments (ref. 7).

Average dwell time is defined as the total amount of time spent looking at an instrument divided by the total number of dwells on that instrument. Percentage of average dwell time is defined as the total dwell time the oculometer had the pilot's eye in track. The sum of the dwell percentages of all the instruments may total to less than 100 percent, since the pilot may look out the window or at his map. The percentage of transitions between two particular instruments is defined as the number of times a pilot's dwell changed between those two instruments divided by the total number of instrument transitions.

The mean and standard deviation were computed for the eye scan data parameters for each of the entire data sets used in the comparisons. The data for the eye scan parameters were combined for all six of the pilots. In this report, the eye scan data were interpreted taking into context the difficulty of

the task, the available situation information, tracking performance, and pilot comments.

Pilot comments were recorded that could help define guidance and situation information requirements, approach path geometrical constraints, and pilot acceptance of curved approach paths for normal airline operations. The pilots also made comments about the approach chart formats used during this test. These comments were summarized in a separate section of this report.

Results and Discussion

Flight Director Guidance Comparison

In this section of the paper, differences are discussed between the computed performance statistics for various data groups with the flight director turned on and with the flight director turned off. The purpose of this comparison was to determine whether flight director guidance should be a requirement for commercial jet transports that are manually flown on curved paths during an approach to landing. Five data sets selected from table II were used to make this comparison.

The first data set (table II, set 2) in this comparison contained test runs flown on the curved paths with the flight director turned off. During these test runs, only the segmented algorithm was used to provide inputs for the HSI.

The second data set (table II, set 5) contained test runs flown on curved paths with the flight director turned on. This data set was limited to test runs using only the segmented algorithm for inputs to the HSI so that differences due to the situation information algorithms would be eliminated.

The third data set (table II, set 1) of this comparison contained only test runs flown with the flight director on, but included test runs (including those used in the second data set) using all three situation information algorithms to provide inputs to the HSI.

The last two of the five data sets contained test runs flown on the SLINE approach (straight-in path, 5 to 6 miles in length). These data sets illustrated the performance expected during a typical ILS approach. One data set (table II, set 3) was flown with the flight director on and the other set (table II, set 4) with the flight director off.

Path tracking data—flight director on versus off. Table III shows the path tracking error information from the five data sets used to assess the need for flight director guidance for curved approach paths. Figure 14 shows a bar plot of the average of

Table III. Effect of Flight Director Usage on Path Tracking Errors

[Flight director on and off]

		Curved paths			Straight-in path	
		Segmented algorithm		All algorithms	Segmented algorithm	
		Flight director off (45 test runs)	**Flight director on** (60 test runs)	**Flight director on** (176 test runs)	**Flight director off** (12 test runs)	**Flight director on** (50 test runs)
Lateral tracking error, total path, ft	Average of rms values	833.1	63.9	68.2	187.2	12.0
	Std. dev. of rms values	756.4	80.9	95.7	41.7	6.5
Track angle error, total path, deg	Average of rms values	7.3	1.4	1.5	2.9	0.5
	Std. dev. of rms values	3.7	1.0	1.2	0.5	0.3
Vertical error, total path, ft	Average of rms values	87.5	33.9	33.5	56.8	35.6
	Std. dev. of rms values	36.0	14.4	12.7	16.0	32.1
Lateral tracking error, 200−ft decision height, ft	rms	273.7	16.6	25.2	109.7	9.7
Vertical tracking error, 200−ft decision height, ft	rms	48.2	21.0	17.0	19.3	12.2
Vertical speed, 200−ft decision height, ft/min	Average	−858	−764	−737	−996	−785
	Std. dev.	347.1	188.6	178.2	139.9	167.5
Touchdown distance on runway, ft	Average	1941	1531	1481	1018	1554
	Std. dev.	612.1	530.2	515.4	224.9	417.1

the rms values from table III of the lateral and vertical path tracking errors for the entire path length and when the decision height point was crossed.

A comparison of the average of the rms values of path tracking errors for the entire curved path length indicates a substantial improvement in tracking with the use of the flight director. On the curved paths, the use of the flight director reduced the rms value of the lateral path tracking errors from 833.1 ft to 63.9 ft (segmented algorithm only) and to 68.2 ft (all algorithms). Respective reductions of the standard deviations of these data (shown in table III) were from 756.4 ft to 80.9 ft (segmented algorithm only) and to 95.7 ft (all algorithms), which indicated an improvement of path tracking consistency with the use of the flight director.

Flight director guidance reduced the average of the rms values of the track angle error (table III) from 7.3° to 1.4° (segmented algorithm) and to 1.5° (all algorithms) on the curved path sets. This reduction indicates that a more consistent, or stabilized, approach was flown with the use of the flight director.

Similar indications of improvements to the vertical tracking performance and consistency with the use of the flight director are also shown in figure 14

and table III. The use of flight director guidance reduced the average of the rms values of the vertical path errors from 87.5 ft to 33.9 ft (segmented algorithm) and to 33.5 ft (all algorithms). The standard deviations (table III) were changed from 36.0 ft to 14.4 ft and to 12.7 ft, respectively. On a relative basis, these reductions are greater than an order of magnitude in both cases.

For the straight-in (SLINE approach) path, the magnitudes of the average of the rms values of the lateral path tracking errors were less than on the curved paths. This was expected because less maneuvering is required along the path. The use of flight director guidance on the straight-in path reduced the average of the rms values of the lateral path tracking errors from 187.2 ft to 12.0 ft. The standard deviations of the rms values of the lateral path tracking errors were reduced from 41.7 ft to 6.5 ft using the flight director. Table III also shows that the average of the rms values of the track angle errors was reduced from 2.9° to 0.5°. As on the curved paths, it was concluded that use of the flight director improved the lateral path tracking performance.

The use of flight director guidance reduced the average of the rms values of the straight-in path vertical tracking deviations from 56.8 ft to 35.6 ft.

Table IV. Effect of Flight Director Usage on Control Activity

[Flight director on and off]

		Curved paths			Straight-in path	
		Segmented algorithm		All algorithms	Segmented algorithm	
		Flight director off (45 test runs)	**Flight director on** (60 test runs)	**Flight director on** (176 test runs)	**Flight director off** (12 test runs)	**Flight director on** (50 test runs)
Column input rate, inputs/min	Average	24.8	19.6	19.1	21.7	14.3
	Std. dev.	13.8	13.0	11.7	7.7	9.6
Column input reversal rate, inputs/min	Average	11.8	9.5	9.3	9.7	7.2
	Std. dev.	6.6	6.2	5.9	3.4	4.6
Wheel input rate, inputs/min	Average	174.0	170.1	171.0	202.0	148.3
	Std. dev.	27.1	34.6	33.6	29.8	48.6
Wheel input reversal rate, inputs/min	Average	56.0	52.7	51.7	61.3	47.5
	Std. dev.	12.7	12.4	12.5	9.8	14.7

However, the standard deviations for these averages were 16.0 ft and 32.1 ft, respectively. It was anticipated that the standard deviation would have been lower with the use of the flight director.

A review of the test run data showed that 3 of the 50 test runs using the flight director had an rms vertical path tracking error, for the total path, exceeding 100 ft. The test subjects who flew these runs commented that they did not usually fly a "tight" approach until closer to the decision height if they felt they could null the tracking errors easily, such as with the use of the flight director. All three of these runs were completed with a successful landing. If these three test runs are not considered in the flight-director-on computations, the average of the rms vertical tracking errors would be reduced from 35.6 ft to 28.9 ft and the standard deviation reduced from 32.1 ft to 16.1 ft.

The lateral and vertical path tracking errors at the decision height, shown in table III and figure 14, are similarly reduced with the use of the flight director. On the curved paths, the use of the flight director guidance reduced the decision height lateral path tracking error from 273.7 ft to 16.6 ft (segmented algorithm) and to 25.2 ft (all algorithms). The decision height vertical path tracking error was decreased from 48.2 ft to 21.0 ft (segmented algorithm) and to 17.0 ft (all algorithms).

The averages and standard deviations of the vertical speed of the airplane at the 200-ft AGL decision height point and of the touchdown point on the runway, shown in table III, were consistent when the flight director was used on the curved paths. These data indicated a consistency in the stability in which the approaches were flown. These same data were greater when the flight director was not used on the curved paths. This indicated, as expected, that somewhat fewer stabilized approaches were flown on the curved paths.

However, when no flight director was used on the straight-in path, the data indicated a greater degree of stabilization. This was not expected and a reason for this result is not apparent.

For the 45 test runs in the curved path, flight-director-off data set, 37 were completed to landing and 8 had missed approaches executed by the pilot. For the other two curved path data sets where the flight director was used (60 and 176 test runs), no missed approaches were caused by tracking errors. All the test runs on the straight-in path, both with and without the use of the flight director, were completed with a landing.

Control activity—flight director on versus off. Table IV shows the control column and wheel activity information from the five data sets. Figure 15 shows a bar plot of the average and standard deviation of the wheel and column inputs and reversals for each of the data sets listed in table IV. The average wheel and column input rates were approximately proportional to the average wheel and column reversal rates for all the data sets. Wheel reversals were between 30 to 32 percent of the wheel inputs. Column reversals were between 45 to 50 percent of the column inputs.

Table V. Effect of Flight Director Usage on Pilot Eye Scan Dwell Time

[Flight director on and off]

		Curved paths			Straight-in path	
		Segmented algorithm		All algorithms	Segmented algorithm	
		Flight director off (45 test runs)	**Flight director on** (60 test runs)	**Flight director on** (176 test runs)	**Flight director off** (12 test runs)	**Flight director on** (50 test runs)
Percent dwell time	ADI	41.0	59.2	59.3	54.1	59.6
	HSI	17.4	4.3	4.0	21.9	3.0
	Airspeed indicator	4.2	4.9	5.0	5.2	5.2
	Altimeter	3.5	2.2	2.4	3.9	3.4
	Engine instruments	0.9	1.7	1.8	0.5	2.0
	VSI	2.8	1.5	1.4	2.1	2.5
	Others	11.3	6.3	8.2	4.1	5.5
Percent total instrument dwell time		81.2	80.1	82.1	91.8	81.2
Average dwell time, sec	ADI	0.91	1.52	1.54	1.41	1.5
	HSI	0.77	0.39	0.39	1.11	0.38
	Airspeed indicator	0.53	0.46	0.46	0.67	0.48
	Altimeter	0.43	0.38	0.39	0.51	0.41
	Engine instruments	0.71	0.75	0.83	0.82	0.83
	VSI	0.35	0.29	0.29	0.47	0.36

The data also show that on the straight-in path, the use of flight director commands reduced the average wheel input rate 27 percent—from 202.0 to 148.3 inputs/min. However, this was not the case for the curved paths.

For the curved path tests, the rate was only dropped approximately 2 percent—from 174.0 to 170.1 (segmented algorithm, 2.2 percent) and to 171.0 (all algorithms, 1.7 percent). This small reduction was attributed to the fact that the segmented algorithm displayed only a full-scale lateral path deviation to the pilot. As such, having no flight director steering commands, the test subjects simply held the airplane in a constant bank angle while turning to an intercept heading for the next straight leg. This resulted in a reduction of wheel inputs during turns. Although the wheel input rate was reduced during the turns, it increased during the capture of the straight segment after the turn. This resulted in a small net change in wheel inputs, with or without flight director steering commands.

The column input rate was somewhat higher on both the curved path data sets and the straight-in path sets when the flight director was not used. This was expected, since the pilot had to find the correct airplane pitch attitude by trial and error as

the trim and pitch attitude requirements for stabilized flight changed because of lateral maneuvering, airspeed and thrust changes, and airplane configuration changes. When the flight director steering commands were used, the column activity was reduced 21–23 percent on the curved paths and 34 percent on the straight-in path. This was expected, since the flight director would command the correct pitch attitude to the pilot, resulting in fewer trial and error inputs.

It should be noted that all the pilots stated that their perceived workload was significantly higher without the use of the flight director. Based on these data and the pilot comments, it was concluded that flight director guidance would reduce the physical workload for the pilot.

Eye scan—flight director on versus off. Table V shows the percent of dwell time and the average dwell time that the pilot looked at the major flight instruments in the cockpit while flying on both the curved paths and the straight-in path, with and without the use of the flight director.

Flight director steering commands are a compelling form of guidance and, as such, demand a large amount of the pilot's attention. As expected, when the flight director was off, the pilot's eye scan

pattern and the manner in which the pilot used the flight instruments changed substantially for both the curved paths and the straight-in path. While flying the curved paths with the flight director on, the subject pilots viewed the center of the ADI (where flight director steering bars and the airplane attitude reference symbol are collocated) 59.2 (segmented algorithm) and 59.3 (all algorithms) percent of the time. When the flight director was off, it was viewed 41 percent of the time.

The reduction of time spent looking at the ADI with the flight director allowed the pilot to look at other flight instruments. A substantial increase in percent of dwell time on the HSI was noted: 4.3 percent (segmented algorithm) and 4.0 percent (all algorithms) with the flight director on and 17.4 percent with the flight director off. Smaller increases, but statistically significant (Probability < 0.01), also occurred on the altimeter and the vertical speed indicator.

There was, however, a small decrease in percent of dwell time on the airspeed indicator and the engine instruments when the flight director was off. It is not clear why the pilot paid less attention to the airspeed indicator and the engine instruments when workload increased, since they are primary sources of information for airspeed control. One possible explanation is that with the use of flight director pitch and roll steering commands, more time was available for the pilot to scan the airspeed and engine instruments. Airspeed control was observed to be uniform for the paths with or without the flight director guidance.

The data for percent of dwell time on the various displays, indicators, and instruments while on the straight-in path were similar to those attained on the curved paths except that the percent of dwell time on the ADI was only reduced from 59.6 to 54.1. However, the percent of total instrument dwell time was proportionately greater. This indicates that the pilot spent a greater amount of time looking at the flight instruments and less time looking out the windows or at the map with the flight director off.

For curved path data sets, the average dwell time spent on the center of the ADI decreased from 1.52 sec (segmented algorithm) and 1.54 sec (all algorithms) to 0.91 sec when the flight director steering bars were turned off. However, the dwell time on the HSI increased from 0.39 sec (segmented algorithm) and 0.39 sec (all algorithms) to 0.77 sec. These changes indicate the importance of the lateral steering commands given by the flight director and the increased importance of the HSI when the

lateral steering command bar was removed. The average dwell times for all other instruments except the engine instruments increased slightly.

The percent of eye scan transitions between the instruments changed significantly with the use of flight director steering commands. With the flight director on, the scan was a hub-and-spoke pattern with the hub centered on the ADI. Eighty-five percent of the total number of instrument transitions were made to or from the ADI. Sixteen percent of the total number of transitions were made between the HSI and the ADI, and another two percent were made between the HSI and all other instruments.

When the flight director was shut off, the eye scan became more of a two-hub pattern with the second hub centered on the HSI. Seventy-five percent of the total number of transitions were made to or from the ADI. Twenty-three percent of the total transitions were made between the HSI and the ADI, and another 10 percent were made between the HSI and all the other instruments. There also were additional instrument transitions between the altimeter and the vertical speed indicator and between the HSI and the vertical speed indicator when flight director guidance was used.

Discussions with the pilots and a review of the instrument scan data have shown that when flight director guidance was used, the pilot could satisfy steering commands with the proper pitch and roll inputs and check that airplane performance was within acceptable bounds through quick glances at the flight instrumentation. Without the use of flight director guidance, the pilot was forced to gather specific performance information (airplane heading, altitude, vertical speed, lateral and vertical path tracking errors, etc.) from a variety of flight instruments so that the necessary roll and pitch inputs could be made. With the flight director off, the pilot's scan pattern indicated a higher visual workload.

Summary—flight director on versus off. Statistical data for path tracking errors, control activity, and pilot eye scan patterns were compared with the flight director on and off. The comparison showed that path tracking errors were smaller with the flight director on for curved approach paths. The pilot's eye scan percent dwell time on instrumentation indicated that the scan patterns changed. The scan pattern with the flight director off indicated a higher visual workload than with the flight director on. Based on these results, the use of flight director steering commands is recommended to manually fly complex curved approach paths for a commercial jet airplane with electromechanical instrumentation.

Table VI. Path Tracking Errors and Touchdown Distance for the Three Situation
Information Guidance Algorithms

[Flight director on]

		Segmented algorithm (60 test runs)	Circular, fixed radius algorithm (58 test runs)	Circular, computed radius algorithm (59 test runs)
Lateral tracking error, total path, ft	Average of rms values	63.9	86.5	58.0
	Std. dev. of rms values	80.9	131.9	61.3
Track angle error, total path, deg	Average of rms values	1.4	1.7	1.3
	Std. dev. of rms values	1.0	1.6	1.0
Vertical tracking error, total path, ft	Average of rms values	33.9	34.2	33.0
	Std. dev. of rms values	14.4	9.8	14.1
Lateral tracking error, 200-ft decision height, ft	rms	16.6	18.3	36.0
Vertical tracking error, 200-ft decision height, ft	rms	21.0	16.3	17.2
Vertical speed, 200-ft decision height, ft/min	Average	−737	−788	−767
	Std. dev.	178.2	197.0	185.4
Touchdown distance on runway, ft	Average	1481	1662	1454
	Std. dev.	515.4	529.8	520.5

Situation Information Algorithm Comparison

The purpose of this comparison was to determine differences in tracking performance and pilot workload due to the algorithm design and situation information presentations. Only test runs flown on curved paths with the flight director on were used in the comparison. Three data sets were used. One data set (table II, set 5) contained only test runs with the segmented algorithm, the second set (table II, set 6) with only the circular, fixed radius algorithm, and the third set (table II, set 7) with only the circular, computed radius algorithm.

Of specific interest in the comparisons of these three data sets were the differences due to the segmented versus continuous path situation information displayed on the HSI, the computed versus specified radius for each turn, and the single-step versus the two-step vertical path transitions. Comparisons were made between the three data sets, each containing only one type of situation information algorithm.

Path tracking data—situation information algorithm comparison. Table VI shows the path tracking error information from the three data sets used in the situation algorithm comparison. Figure 16 shows a bar plot of the average of the rms

values of the lateral and vertical path tracking errors for the entire path length and when the decision height point was crossed.

The averages of the rms lateral tracking errors for the three algorithms differed by less than 28.5 ft (less than the width of a typical runway). The average and standard deviation of the rms track angle errors were small, which indicated that lateral tracking was stable. The average and standard deviation of the rms vertical tracking errors were almost the same for all situation information algorithms. This indicates that either the single-step or the two-step vertical transition would be flyable.

However, pilot comments indicated that the use of the segmented algorithm, which is based on capturing the next straight path segment, may not be acceptable. The pilots were concerned that the full-scale lateral deflections that resulted during turns would not allow the pilot to know whether the aircraft was tracking on course or had large lateral errors.

All approaches in each data set were completed with a landing. The averages and standard deviations of the vertical speed of the airplane at the 200-ft AGL decision height and of the touchdown point on the runway were consistent between each of the

13

Table VII. Control Activity for the Three Situation Information Guidance Algorithms

[Flight director on]

		Segmented algorithm (45 test runs)	Circular, fixed radius algorithm (60 test runs)	Circular, computed radius algorithm (176 test runs)
Column input rate, inputs/min	Average	19.6	18.8	19.3
	Std. dev.	13.0	11.9	10.7
Column input reversal rate, inputs/min	Average	9.5	9.0	9.6
	Std. dev.	6.2	6.0	5.4
Wheel input rate, inputs/min	Average	170.1	168.5	175.3
	Std. dev.	35.6	34.4	31.8
Wheel input reversal rate, inputs/min	Average	52.7	51.4	51.4
	Std. dev.	12.4	12.2	13.1

Table VIII. Pilot Eye Scan Dwell Time for the Three Situation Information Guidance Algorithms

[Flight director on]

	Instruments	Segmented algorithm	Circular, fixed radius algorithm	Circular, computed radius algorithm
Percent dwell time	ADI	59.2	60.5	58.2
	HSI	4.3	4.1	3.6
	Airspeed indicator	4.9	5.0	5.1
	Altimeter	2.2	2.3	2.6
	Engine instruments	1.7	1.8	1.9
	VSI	1.5	1.4	1.3
	Other instruments	6.3	6.6	8.6
Percent total instrument dwell time		80.1	81.7	81.3
Average dwell time, sec	ADI	1.52	1.62	1.48
	HSI	0.39	0.39	0.38
	Airspeed indicator	0.46	0.46	0.46
	Altimeter	0.38	0.36	0.42
	Engine instruments	0.75	0.79	0.95
	VSI	0.29	0.29	0.29

algorithms. These data indicated a consistency in the stability in which the approaches were flown with each of the algorithms.

Control activity—situation information algorithm comparison. Table VII shows the control column and wheel activity information from the three data sets. Figure 17 shows a bar plot of the averages and standard deviations of the wheel and column inputs and reversals for each of the data sets listed in table VII. These data show virtually no differences in control activity between the three situation information algorithm data sets. The magnitudes of the input rates and the reversal rates were the same as those found in figure 15 and table IV for the curved path data set with the flight director on.

Eye scan—situation information algorithm comparison. Table VIII shows the percent of dwell time and the average dwell time that the pilot looked at the major flight instruments in the cockpit for the situation information guidance data sets.

The eye scan data shown in table VIII reveal no major differences in the instrument scan pattern or manner in which the instruments were used by the pilot due to the difference between the situation information algorithms. The percent of dwell time on the ADI ranged between 58 percent and 60 percent for the three algorithms.

Summary—situation information algorithm comparison. Lateral and vertical path

Table IX. Path Tracking Errors and Touchdown Distance for the Four Approaches

[Flight director on]

		HOOK approach (59 test runs)	RIVER approach (61 test runs)	OFFSET approach (57 test runs)	SLINE approach (50 test runs)
Lateral tracking error, total path, ft	Average of rms values	34.9	62.0	112.8	12.0
	Std. dev. of rms values	24.1	56.6	147.4	6.5
Track angle error, total path, deg	Average of rms values	0.8	1.6	2.0	0.5
	Std. dev. of rms values	0.4	1.0	1.7	0.3
Vertical tracking error, total path, ft	Average of rms values	36.8	29.7	34.8	35.6
	Std. dev. of rms values	13.3	11.9	12.6	32.1
Lateral tracking error, 200-ft decision height, ft	rms	10.4	39.7	13.3	9.7
Vertical tracking error, 200-ft decision height, ft	rms	17.9	18.3	18.8	12.2
Vertical speed, 200-ft decision height, ft/min	Average	−735	−754	−804	−758
	Std. dev.	177.6	187.9	191.9	167.5
Touchdown distance on runway, ft.	Average	1461	1688	1436	1554
	Std. dev.	529.6	536.4	482.7	417.1

tracking error data, control wheel and column activity, and pilot eye scan data indicated no preference to the type of situation information, with flight director steering commands, that should be required to fly the curved paths. However, pilot comments indicated that the segmented algorithm may not be desirable, since the lateral path error indications are full-scale during most turns.

Approach Path Comparison

The purpose of this comparison was to determine which geometrical path characteristics could detrimentally affect tracking performance or change pilot workload. Geometric characteristics of specific interest included the magnitude of turn radii, time or distance between consecutive turns, and length of the final straight-in segment to the runway.

The approach path comparison was made between four data sets, each containing only approaches of one type of the three curved paths (OFFSET [table II, set 10], RIVER [table II, set 8], and HOOK [table II, set 9] approaches) or the straight-in path (SLINE [table II, set 3] approach). Each of the curved path data sets was composed of approaches using all the situation information algorithms and flown with flight director guidance. The straight-in approach data set used only the segmented algorithm with the flight director on.

Table IX shows the path tracking error information from the four data sets used to evaluate the geometric path characteristics. Figure 18 shows the average of the rms values of the lateral and vertical path deviations for the entire path length and when the decision height point was crossed.

Path tracking data—approach path comparison. The lateral errors and the track angle errors for the entire path length were expected to be functions of the number of turns or path direction changes required in each path. The data shown indicate that this was the case except for the OFFSET approach. In the OFFSET approach, the average and standard deviation for the lateral tracking error were substantially larger than on the other paths even though it had fewer turns than the RIVER and HOOK approaches. The track angle error data on the OFFSET approach were also the largest.

A review of the individual OFFSET approach test runs showed that many lateral path errors occurred on the segment of the approach with the two 90° consecutive turns. Fifteen out of 57 of the OFFSET approaches were found to have an rms lateral path tracking error greater than 100 ft. Twelve of those 15 approaches used wind model 2, which led to the following investigation.

15

An investigation of the effects of wind model 2 for the OFFSET approach cases was conducted. The crossing and head wind components of wind model 2 relative to the airplane were computed for the beginning and the end of each of the turns. At the beginning of the first 90° turn to the right, there was a 3-knot head wind component and a 26-knot crosswind component from the left acting on the airplane. As the airplane completed the first turn and started the second 90° turn to the left, the head wind and crosswind components changed significantly because of the 90° track angle change and the altitude change of the airplane. At the end of the first 90° turn, the head wind shifted to a 23-knot tail wind component (26-knot total change) and the crosswind to a 5-knot component from the left (21-knot total change). At the completion of the second turn, the relative wind had again changed to a 7-knot head wind component (30-knot total change) and to a 19-knot left crosswind component (12-knot total change).

The change from a head wind to a tail wind component during the first turn resulted in a higher ground speed and that, in turn, required a constantly increasing bank angle to remain on the path. On completion of the right turn, the pilot had to immediately follow the flight director commands to roll the airplane into the left turn, since there was no straight segment between the turns. If the pilot failed to follow the flight director commands at this point, large lateral errors would rapidly occur. This was also the segment of the OFFSET approach where the pilot was quite busy with flap and landing gear configuration and with completion of the final landing checklist. These events tended to cause momentary distractions from the flight director, which resulted in a buildup of lateral tracking errors.

The nominal bank angles required to fly the airplane during the turns on the OFFSET approach path were within the maximum 25° lateral steering command limit. However, there were only a few degrees of additional steering command margin left to correct for any lateral path error that might have developed. Therefore, if a large error developed, it would require more time to correct.

The two geometric characteristics most apparent with this segment of the OFFSET approach path are the consecutive turns and the large track angle (direction) changes required. In the RIVER approach, the last 5 miles of the path contains four virtually consecutive turns, and the pilots experienced few problems remaining on that path. As can be seen from the data, the lateral path tracking error was less than 62 ft on the RIVER approach. However, the largest track angle change was 49°, thus reducing

adverse effects of wind changes due to the airplane turning.

Large track angle changes (up to 90°) were also in the HOOK approach but with a straight segment between the turns. This resulted in relative wind shifts similar to those encountered on the OFFSET approach to also be encountered on the HOOK approach. However, large lateral tracking errors that occurred on the OFFSET approach did not occur on the HOOK approach. It was concluded that the larger lateral errors for the OFFSET approach were the result of the consecutive turns with no straight segment in between, coupled with the large track angle change and the adverse wind conditions during the turns.

The winds adversely affected the capability of the flight director to correct lateral path errors by increasing the ground speed (greater bank angle required to fly on the path) and by causing lateral drift of the airplane relative to the path. Without the straight segment between the turns, the pilot had no opportunity to correct the lateral error that had developed. This problem may be reduced by requiring larger turn radii and/or by requiring a short straight segment between turns as in the HOOK approach.

The average of the rms values of the vertical path deviations for each of the data sets was approximately the same for each of the approaches. Note that the standard deviation of the vertical tracking error was largest on the SLINE approach. One explanation for this is that, since the SLINE approach path was a straight line and relatively easy to fly, the pilots felt that the approach could be flown with a larger tolerance for path tracking error until approaching the decision height point where tracking accuracy was more critical. This larger tolerance would result in less pilot workload and a smoother ride. The decreased lateral and vertical path deviations at the decision height point support this explanation.

The rms value of the lateral tracking error for the RIVER approach at the decision height point was 40 ft. This is believed to be caused by the decision height point being located at the end of the last turn—a 37° track angle change. Although this lateral path deviation was within the width of the runway, the subject pilots felt that either a final path segment longer than ½ mile or a higher decision height would be required for this approach. The lateral deviations for the remaining approaches and the vertical deviations on all the approaches at the 200-ft AGL decision height point were judged to be acceptable. The 2- and 3-mile-long final straight-in path segments

Table X. Control Activity for the Four Approaches

[Flight director on]

		OFFSET approach (59 test runs)	RIVER approach (61 test runs)	HOOK approach (57 test runs)	SLINE approach (50 test runs)
Column input rate, inputs/min	Average	16.9	20.4	20.5	14.3
	Std. dev.	11.3	11.8	12.1	9.6
Column input reversal rate, inputs/min	Average	8.3	9.9	9.8	7.2
	Std. dev.	5.8	5.8	5.9	4.6
Wheel input rate, inputs/min	Average	162.0	181.3	170.2	148.3
	Std. dev.	33.2	29.4	35.6	48.6
Wheel input reversal rate, inputs/min	Average	50.9	52.4	52.1	47.5
	Std. dev.	11.9	12.4	13.4	14.7

after a 90° track angle change were judged by the pilots to be more than adequate.

The averages and standard deviations of the vertical speed of the airplane at the decision height point, shown in table IX, for all the approaches were within a normal range. This indicated that a fairly stable approach had been flown in the vertical axis.

The average and standard deviation for the touchdown distance from the approach threshold of the runway were as expected. In general, the landing distance average and standard deviation of the paths were much the same with slightly less variation with the easier SLINE approach and slightly longer and more variable with the more complex RIVER approach.

Control activity—approach path comparison. The average and standard deviation of the wheel and column activity during each approach are shown in table X and figure 19.

The wheel input rate was slightly higher on the RIVER approach than on the others. This was expected, since there were more path direction changes in that procedure. Wheel input rate was lowest on the SLINE approach, since there were no turns required. Column input rate was slightly higher on the RIVER and OFFSET approaches. This may have been induced by the increased lateral maneuvering for these approaches.

The control activity to fly on the curved paths was slightly higher than for the SLINE approach, but judged by the pilots to be acceptable.

Eye scan—approach path comparison. Table XI shows the percent of dwell time and the average dwell time that the pilot looked at the major

flight instruments in the cockpit while flying on the three curved paths and the straight-in path.

The eye scan data for the SLINE approach were first compared with the data for each of the curved paths. Then, the eye scan data for each of the curved paths were compared with each other.

The eye scan data indicated that the subject pilots had a 59- to 60-percent dwell time on the ADI for each of the approach paths. However, there were changes in the percent of dwell time on the other instruments between test runs when the SLINE approach was flown and test runs when the curved paths were flown. The percent of dwell time decreased slightly on the vertical speed indicator (2.4-percent SLINE approach to approximately 1.4-percent curved paths) and on the altimeter (3.4-percent SLINE approach to approximately 2.4-percent curved paths). The percent of dwell time increased on the HSI (3.0-percent SLINE approach to approximately 4-percent curved paths) and on the along track DME meter (0.25-percent SLINE approach to 0.5-percent curved paths). The increase in attention to the HSI is attributed to the track angle changes of the curved path and to the along track DME instrument being used for path orientation.

The main difference in the eye scan patterns between the curved paths was exhibited on the RIVER approach. During this approach, the percent of dwell time was greatest on the HSI (4.7 percent) and lowest on the airspeed indicator (4.5 percent). These results conform to the trends in eye scan pattern previously discussed in the flight director on versus off comparison.

Summary—approach path comparison. The lateral and vertical path tracking errors indicate that

Table XI. Pilot Eye Scan Dwell Time for the Four Approaches

[Flight director on]

	Instruments	OFFSET approach	RIVER approach	HOOK approach	SLINE approach
Percent dwell time	ADI	59.8	59.4	58.8	59.6
	HSI	3.5	4.7	3.8	3.0
	Airspeed indicator	5.2	4.5	5.3	5.2
	Altimeter	2.5	2.0	2.6	3.4
	Engine instruments	2.0	1.7	1.8	2.0
	VSI	1.3	1.3	1.6	2.5
	Other instruments	7.7	7.7	9.0	5.5
Percent total instrument dwell time		82.0	81.3	83.0	81.2
Average dwell time, sec	ADI	1.59	1.55	1.48	1.50
	HSI	0.37	0.40	0.39	0.38
	Airspeed indicator	0.47	0.45	0.46	0.48
	Altimeter	0.37	0.37	0.41	0.41
	Engine instruments	0.92	0.79	0.78	0.83
	VSI	0.30	0.28	0.28	0.36

all the curved approaches could be flown as a precision approach. However, complex paths with short straight segments, such as on the RIVER approach, may require longer final leg segments and/or higher landing minima.

Pilot workload was higher on the curved approaches, as indicated by the control activity and variation in the touchdown point on the runway. Adverse winds may require a straight path segment between consecutive large angle change turns and/or the use of larger turn radii.

If flight director steering commands are not used, then the decision height should be increased and the relatively large lateral path tracking errors considered in the design of the approach procedure.

Pilot Comments

The following section summarizes the comments made by the pilots during and just after each approach and during a final debriefing after all the approaches were completed. The comments recorded in the final debriefing were particularly pertinent, since the pilots had just flown numerous approaches and had time to formulate their opinions of the situation information and approach procedures.

Acceptability. The following comments reflect the acceptability and concerns of manually flying a jet transport airplane along curved approach paths during airline operations.

All the test subjects indicated that all the curved path approach procedures manually flown during the evaluation tests were acceptable for normal airline operations provided flight director guidance was used. Without flight director guidance, flying curved approaches in a jet transport airplane would require much greater training and use of nonprecision-approach landing minima. The pilots emphasized the requirement of flight director command guidance to fly curved precision-approach paths. This requirement was also supported by the path tracking data.

The pilots reported that when flying on the curved approach paths, their perceived workload was higher than when flying a conventional straight-in ILS approach, but less than when flying a typical nonprecision approach. The trends in the eye scan data and the control activity data support the difference in perceived workload between the curved and the straight-in paths.

The pilots also felt that the curved approach paths would require more cockpit briefing and crew training than for an ILS approach. One test subject suggested that a pilot might have to be certified for a particular approach. Certification, in this case, would mean that the pilot had flown the approach procedure during a training period in a simulator or had flown the actual procedure under the supervision of another pilot previously certified for the approach.

Situation information preferences. All the pilots stated that they could use any of the path

guidance algorithms to fly the curved paths if flight director commands were also used. This was supported by the eye scan and path tracking data.

However, several pilots voiced a strong concern about using the segmented algorithm situation information when the lateral-path-deviation indicator was deflected full-scale (which occurred regularly during a turn). They felt that even though the flight director was providing commands to fly a designated curved path, the flight crew could not determine whether they were on track or had a large lateral error. One pilot pointed out that if there was a large lateral error, he could be satisfying the flight director commands to return to course and actually be guided into an obstacle.

At the end of the data collection approaches, the pilots were given the opportunity to fly several approaches with either of the circular path algorithms without the use of the flight director. They were then asked to comment on the differences between the segmented algorithm and the circular, fixed radius algorithm when the flight director was not used. The pilots agreed that the workload was higher in a turn when the circular, fixed radius path algorithm was used. This was to be expected, since this algorithm displayed the programmed course direction and the lateral path deviations for the pilot to continuously null throughout the turn. However, at the beginning of a turn, the segmented algorithm drove the course select on the HSI to the outbound path direction and computed lateral tracking errors relative to the outbound path segment. The pilot would then simply turn the airplane to an intercept heading until capturing the next path segment. The pilots reported that their anxiety level was higher when the segmented algorithm was full-scale, since they did not know precisely where they were relative to the path.

The pilots were asked to comment on the differences in vertical situation information (i.e., vertical path changes at the midarc of the turn or at both the beginning and the end of the turn). All the pilots indicated that they could easily fly either method of vertical transition. One pilot preferred the midarc transition, four pilots preferred the beginning/end of the turn transition, and one pilot had no preference.

The pilots were also asked to comment on which portions of the situation information were most useful, or not very useful, and what situation information they would like to have that was not included in the evaluation tests. The pilots all agreed that the advance-track-angle arrow on the HSI was a very strong cue that showed the pilot where he was going in the turn.

The pilots felt that along track DME distance to the runway information was very desirable, although it was used for different reasons. Some pilots thought that its prime use would be for letting the pilot know when to configure the airplane for landing. Other pilots used it primarily to determine their progress or location along the path.

The pilots reported that they did not use the relative bearing and distance information of the airplane to the azimuth antenna presented on the RMI and associated DME indicator. The eye scan data also indicated that the pilots rarely observed these instruments. However, these instruments may be beneficial during a missed approach task, and their usefulness should be evaluated in further piloted simulation tests.

Several pilots stated that they would like to have the RMI and the associated DME indicator provide indications relative to the active waypoint instead of the azimuth antenna. They felt that they could better monitor their progress along the path and anticipate turns.

Several pilots also stated that they would like to have an MLS annunciator panel that would show when they had valid azimuth, elevation, and DME signal coverage. They also wanted to annunciate whether the steering commands and the lateral and vertical path deviations were based on area navigation computations or on the "raw" MLS angular signals.

Approach path geometry. The pilots were asked to comment on the geometry of the approach paths tested, specifically about the length of the final straight-in segment, the amount of time (or distance) necessary between turns for airplane stabilization, and the maximum angle of the final turn onto the runway centerline.

The pilots reported that the length of the final straight-in segment was long enough for all approaches. They indicated that the ½-mile final on the RIVER approach required minimal lateral and vertical tracking errors when they rolled out of the turn onto the final straight-in segment.

It should be noted that the final turn on the RIVER approach required a 37° change in path direction. It is not clear that a turn with a larger change of direction would be acceptable with a ½-mile final. The OFFSET and HOOK approaches both had a 90° turn onto the final straight-in segment. The 3-mile and 2-mile final segments on these approaches

19

were reported to be more than adequate to complete the approach successfully.

The RIVER approach and the OFFSET approach each incorporated successive right and left turns with little or no distance between turns for airplane stabilization. The RIVER approach had six turns, four of which occurred in the last 5 miles prior to the runway. The change in path direction on this approach varied between 9° and 49°. The pilots all stated that the successive turns on this approach caused no problems in controlling the airplane or in flying the approach.

However, the pilots indicated that the final 5 miles of the RIVER approach required a very attentive scan of the instrument panel, since there was a large amount of right/left/right maneuvering to fly on the programmed path. Some pilots indicated that they did not have enough time to look at the approach chart and would have to memorize critical information or assign the copilot to make altitude and course direction call outs. All the pilots configured the airplane for landing and completed the final checklist prior to starting the last 5 miles of the RIVER approach.

The OFFSET approach incorporated two consecutive 90° turns with no straight path segment between the turns. One pilot thought that approach was slightly more difficult, but he attributed it to the large (90°) path direction changes required. All the pilots felt that this approach would be acceptable for normal operations.

Approach chart format. Although approach chart formatting was not specifically part of this study, the subject pilots offered comments on the charts used in this study (figs. 5 to 11). Many different individual preferences in the details of the charts were expressed. All pilots expressed satisfaction with the plan view of the approach procedure. None objected to the split plan view of the RIVER approach. One pilot suggested that the profile view be eliminated because he rarely used it; another wanted the profile view to be made larger, since he used it regularly.

All the pilots wanted altitudes printed on the chart that would correspond to the given along track distances. Although the programmed altitude for each waypoint is important for programming the area navigation system, the pilots prefer to have the programmed altitude and along track distance shown at the beginning and end of each turn so that they can cross-check the vertical-path-deviation indications as they progress along the path.

Most pilots wanted the approach chart decluttered by removing waypoint definitions (rho/theta/altitude) relative to the azimuth antenna and removing turn radii indications. They felt that if the area navigation system contained a data base used to define the approach, the waypoint definitions and turn radii could be printed on the back of the chart and used for cross-checking purposes prior to beginning the approach. The pilots also desired that waypoints be defined with names rather than numbers.

General comments. Several of the pilots had flown the actual RIVER approach procedures at the Washington National Airport. Each of these pilots stated that the RIVER approach was much easier to fly with MLS instrument situation information than by using the visual procedures used at Washington National Airport.

Several pilots felt that they could have had smaller path tracking errors if they had been more familiar with the test airplane trim and attitude conditions and power settings for a desired airspeed and descent rate. However, none of the test subjects took the opportunity to fly additional runs offered during the training period.

Concluding Remarks

Six subject pilots flew approximately 60 approaches each, with and without wind and turbulence, to evaluate the use of electromechanical situation information to manually fly on curved paths within the microwave landing system signal environment. Path tracking data, control activity, eye scan patterns of the instrument panel, and pilot comments were used to evaluate (1) flight director versus no flight director guidance, (2) use of three situation information algorithms, and (3) four test paths of different geometric complexity.

In the flight director on versus off comparison, the data showed a substantial reduction of the path tracking errors on the curved paths when flight director guidance was on. Average rms path tracking errors were reduced from 833.1 ft to 63.9 ft laterally and from 87.5 ft to 33.9 ft vertically. No missed approaches were flown when the flight director was on during 176 test runs. Eight missed approaches were flown during 45 test runs when the flight director was off. Pilot comments indicated the need for flight director guidance when flying the curved approaches. Based on these data and comments, it is concluded that flight director guidance is required for manually controlled flight in a jet transport airplane along curved paths to low decision heights

(approximately 200 ft above ground level). Without flight director guidance, much greater pilot training and nonprecision-approach landing minima would be required.

Based upon the path tracking data, control activity, and the eye scan data, virtually no differences in performance were observed between the situation information algorithms when using flight director steering commands. Although the display of information on the horizontal situation indicator was significantly different for the segmented and circular situation information algorithms, the pilots paid the most attention to the flight director. Vertical tracking performance was almost the same for all situation information algorithms, indicating that either the single-step or the two-step vertical transition would be flyable. No difference in eye scan patterns or control activity was noted.

However, pilot comments indicated that the segmented algorithm, which is based on capturing the next straight path segment, may not be acceptable. The pilots were concerned that the full-scale lateral deflections encountered during turns would not allow the pilot to know if the aircraft was tracking on course or had large lateral errors.

During the approach path comparison, pilot comments indicated that all the curved approach paths in these tests could be used in normal airline operations if flight director steering commands were used. The pilots commented that their perceived workload was higher on the curved paths than on a straight-in instrument landing system (ILS) approach, but lower than on a typical nonprecision-approach procedure.

The required length of the straight-in final approach segment of the path, a 200-ft above ground level (AGL) decision height, was influenced by the amount of path direction change (track angle change) required during the last turn onto the final path segment. The lengths of the final straight-in path segment on the curved paths used in this study were 3 miles, 2 miles, and ½ mile. Path tracking data and pilot comments indicated that a 2-mile-long final, when preceded by a 90° turn, was sufficient for a 200-ft AGL decision height. However, path tracking errors for the path with a ½-mile-long final preceded by a 37° turn were larger (although within the width of the runway). If a ½-mile final straight-in path is used, a decision height higher than 200 ft may be required.

NASA Langley Research Center
Hampton, VA 23681-0001
October 7, 1992

References

1. *Getting Ready for MLS.* U.S. Department of Transportation, Jan. 1985.

2. Scott, Barry C.; Goka, Tsuyoshi; and Dargue, Jim: Simulation of MLS-ATC Procedures in the New York and San Francisco Terminal Control Areas. *SAE 1989 Transactions, Journal of Aerospace, Section 1—Volume 98,* 1990, pp. 1301–1330. (Available as 892217.)

3. Parrish, Russell V.; and Bowles, Roland L.: *Motion/Visual Cueing Requirements for Vortex Encounters During Simulated Transport Visual Approach and Landing.* NASA TP-2136, 1983.

4. Lachmann, S. G.; and McKinstry, R. G.: Software Engineering of a Navigation and Guidance System for Commercial Aircraft. AIAA 75-575, Apr. 1975.

5. *Instrument Approach Procedures—U.S. Northeast,* Vol-3 of 3, National Oceanic and Atmospheric Administration, U.S. Dep. of Commerce, June 5, 1986.

6. *Military Specification—Flying Qualities of Piloted Airplanes.* MIL-F-8785C, Nov. 5, 1980. (Supersedes MIL-F-8785B, Aug. 7, 1969.)

7. Harris, Randall L., Sr.; Glover, Bobby J.; and Spady, Amos A., Jr. (appendix A by Daniel W. Burdette): *Analytical Techniques of Pilot Scanning Behavior and Their Application.* NASA TP-2525, 1986.

γ = 0°   WPT04   γ = -1.73°   γ = -2.71°

2300 ft

1827 ft

Begin turn   End turn

Vertical profile view

ADI

HSI

WPT04

Begin turn   End turn

Specified
radius

Oblique view
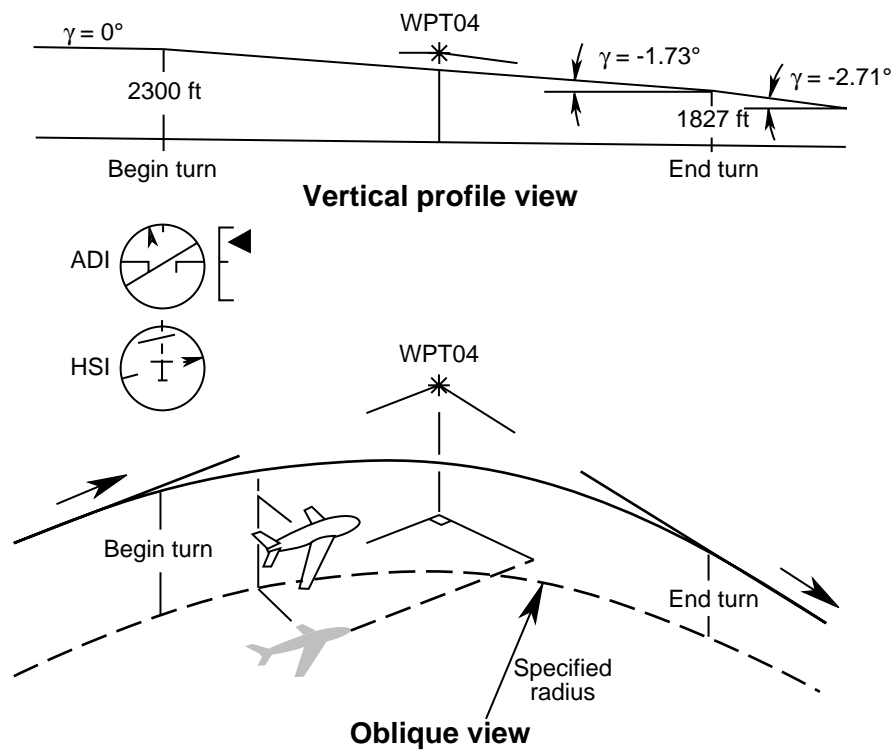
Figure 4. Display format and turn geometry for the segmented algorithm.

γ = 0°   WPT04   γ = -3.1°

2300 ft

1870 ft

Begin turn   End turn

Vertical profile view

ADI

HSI

WPT04

Midpoint
of turn arc

Begin turn

End turn

Specified
radius

Oblique view
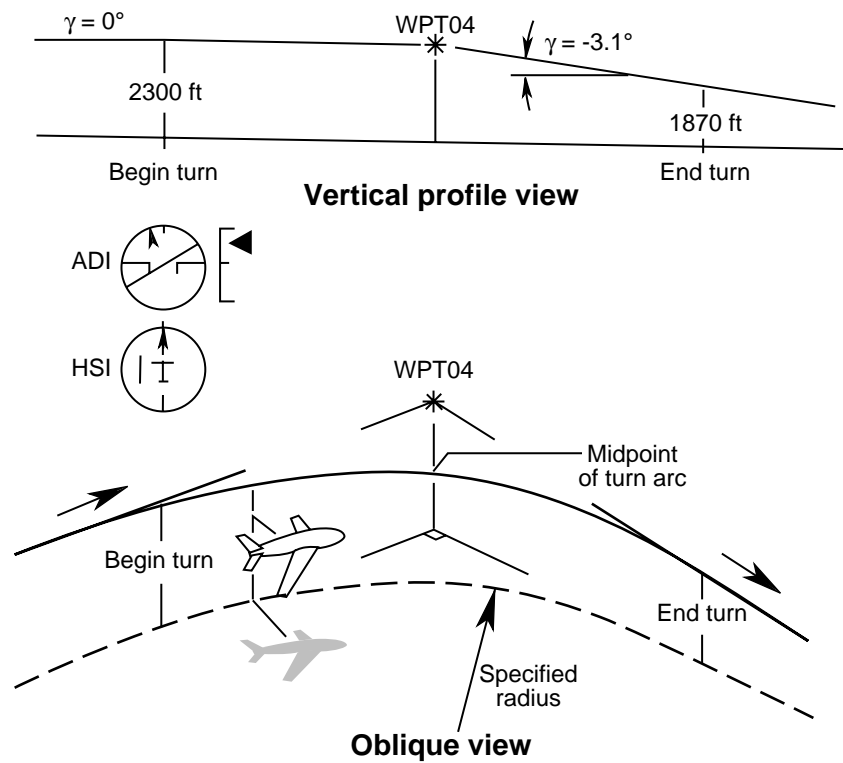
Figure 5. Display format and turn geometry for the circular, fixed radius algorithm.

γ = 0°

WPT04

2300 ft

γ = -1.73°

γ = -2.71°

Begin turn

End turn
(altitude function
of turn radius)

Vertical profile view

ADI

HSI

WPT04

Begin turn

End turn

Computed
radius

Oblique view
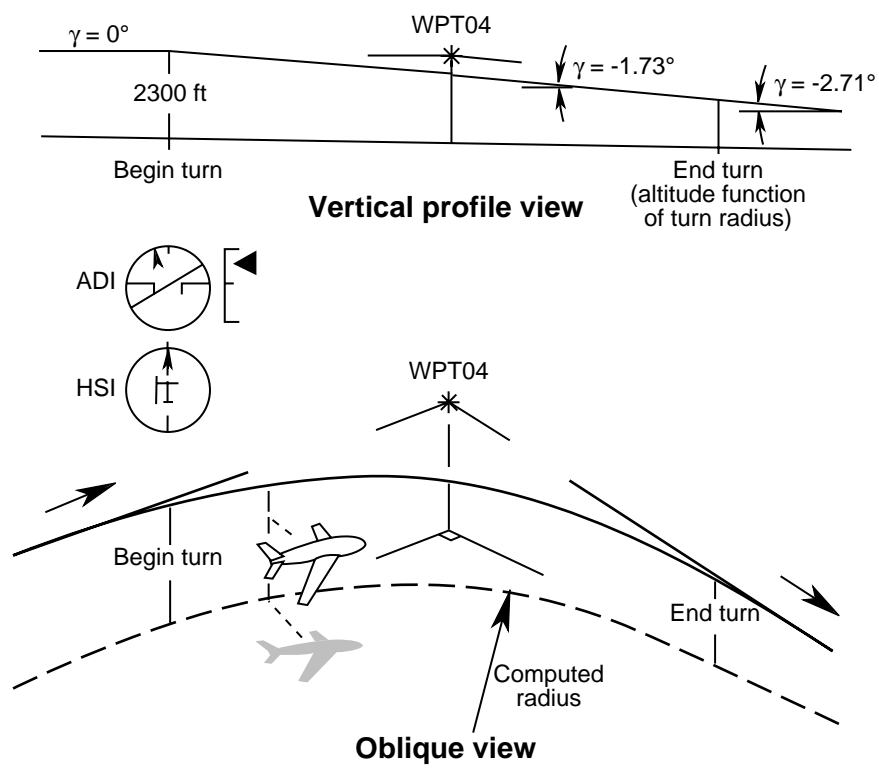
Figure 6. Display format and turn geometry for the circular, computed radius algorithm.

CHINCOTEAGUE ISLAND/WALLOPS FLIGHT FACILITY (WAL)

MLS RNAV RWY 22 SLINE
CHINCOTEAGUE ISLAND, VIRGINIA

PATUXENT APP CON
127.95 314.0
NASA WALLOPS TOWER
126.5 394.3
GND CON
121.7
CLNC DEL 128.25
ATIS 132.65

WPT01
032° -- 30.0
9595
28.1nm

212°

WPT02
032° -- 7.9
1946
6.0nm

212°

WPT03
032° -- 1.9
35

MICROWAVE
Chan 594
M-EZD
DME 110.75 Chan 44 (Y)

MISSED APPROACH
Climbing right turn to 3000
direct to WPT02 and hold.

WPT01

WPT02

212°
9595
1946

6.0nm | 22.1nm

ELEV 41

REIL Rwys 4 and 22
HIRL Rwys 4-22 and 10-28

CATEGORY	A	B	C	D
S-MLS 22	**235-1/2**	200 (200-1/2)		

FOR RESEARCH TESTS ONLY

Knots	60	90	120	150	180
Min:Sec					
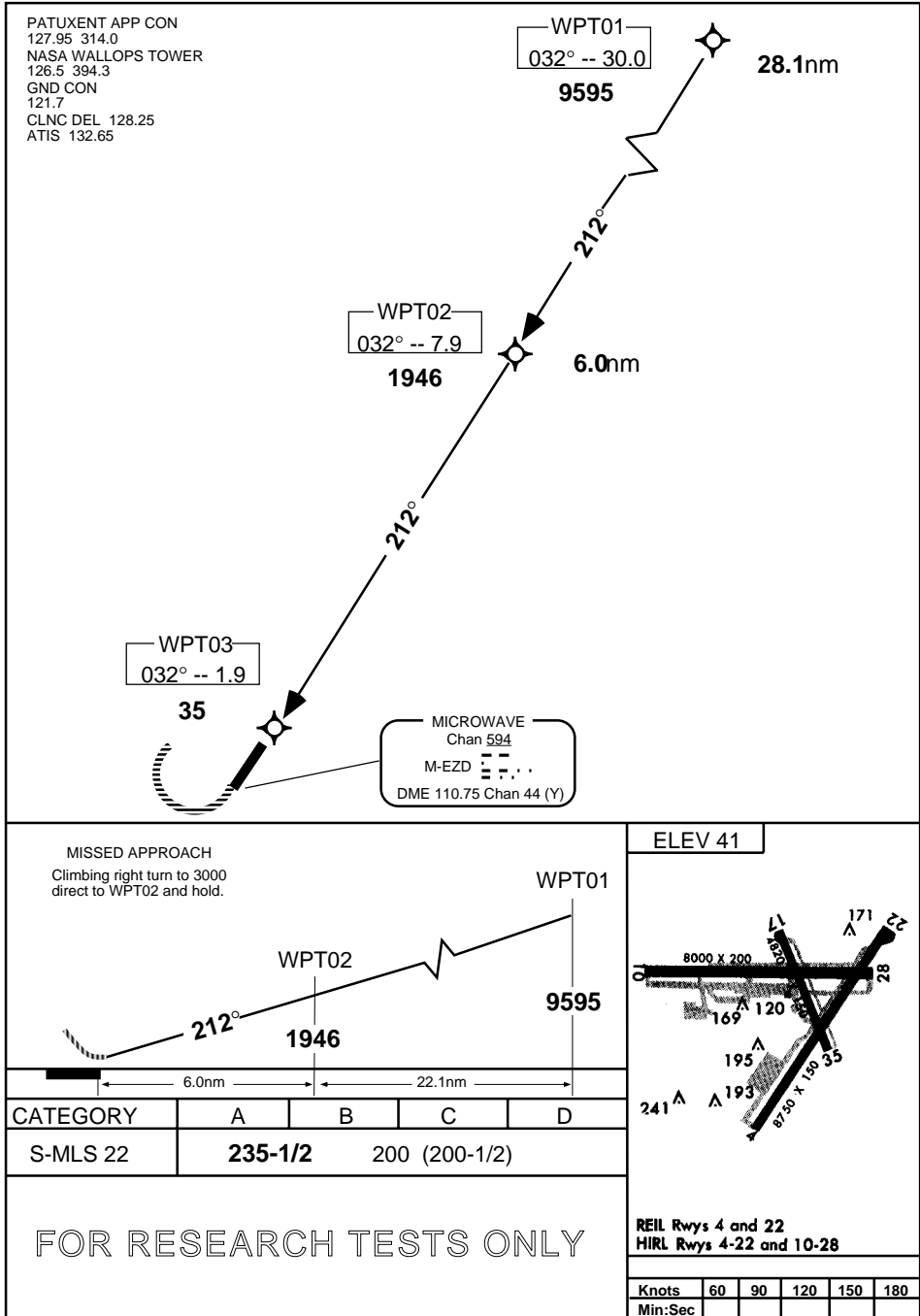
MLS RNAV RWY 22 SLINE
CHINCOTEAGUE ISLAND, VIRGINIA

37° 56'N-75° 28'W   CHINCOTEAGUE ISLAND, VIRGINIA
CHINCOTEAGUE ISLAND/WALLOPS FLIGHT FACILITY (WAL)

Figure 7. ILS straight line (SLINE) approach procedure.

CHINCOTEAGUE ISLAND/WALLOPS FLIGHT FACILITY (WAL)

MLS RNAV RWY 22 OFFSET

CHINCOTEAGUE ISLAND, VIRGINIA

PATUXENT APP CON
127.95 314.0
NASA WALLOPS TOWER
126.5 394.3
GND CON
121.7
CLNC DEL 128.25
ATIS 132.65

WPT01
044° -- 14.1
2300
14.8nm

212°

WPT03
032° -- 6.1
1383
4.2nm

302°

WPT02
058° -- 6.8
2300
7.2nm

212°

WPT04
032° -- 1.9
35

MICROWAVE
Chan 594
M-EZD ▪ ▪▪ ▪ ▪ ▪
DME 110.75 Chan 44 (Y)

MISSED APPROACH

Climbing right turn to 4500
direct to WPT03 and hold.

ELEV 41

WPT02   WPT01

WPT03

212°   x   **2300**   **2300**

1383

| | 4.2nm | 3.0nm | 7.6m | |

CATEGORY	A	B	C	D
S-MLS 22	**235-1/2**	200 (200-1/2)		

FOR RESEARCH TESTS ONLY

REIL Rwys 4 and 22
HIRL Rwys 4-22 and 10-28

Knots	60	90	120	150	180
Min:Sec					

8000 X 200

8750 X 150

171
22
28
35
120
169
195
193
241

MLS RNAV RWY 22 OFFSET

CHINCOTEAGUE ISLAND, VIRGINIA

37° 56'N-75° 28W

CHINCOTEAGUE ISLAND, VIRGINIA
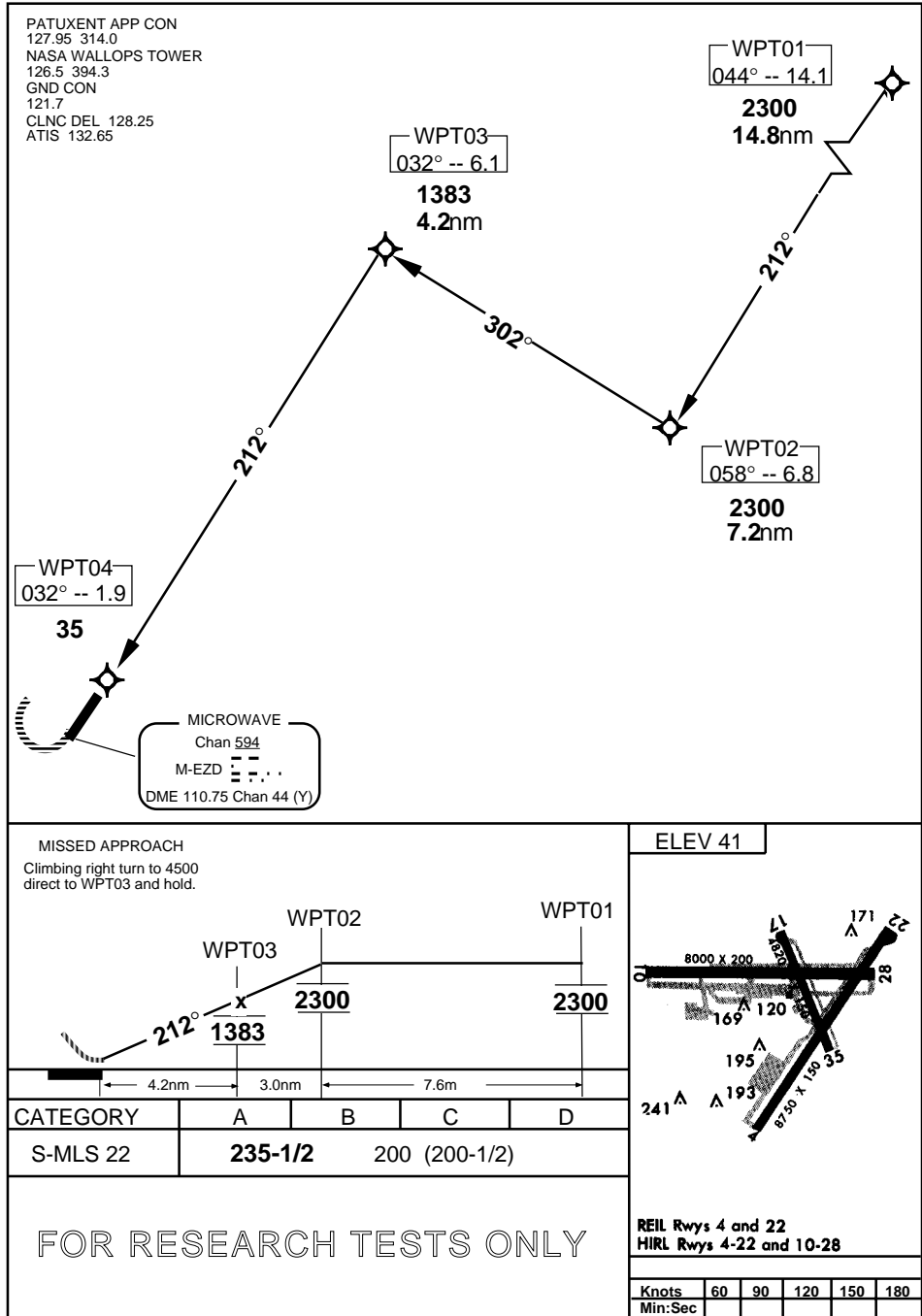CHINCOTEAGUE ISLAND/WALLOPS FLIGHT FACILITY (WAL)

Figure 8. OFFSET approach procedure for segmented algorithm with computed turn radii.

CHINCOTEAGUE ISLAND/WALLOPS FLIGHT FACILITY (WAL)

MLS RNAV RWY 22 OFFSET

CHINCOTEAGUE ISLAND, VIRGINIA

PATUXENT APP CON
127.95 314.0
NASA WALLOPS TOWER
126.5 394.3
GND CON
121.7
CLNC DEL 128.25
ATIS 132.65

WPT01 **13.5**nm
044° -- 14.1
2300

RAD 10000

212°

7.5nm

WPT03
032° -- 6.1
1383

4.9nm

3.0nm

RAD 7500

212°

WPT02
058° -- 6.8
2300

WPT04
032° -- 1.9
35

212°

MICROWAVE
Chan 594
M-EZD
DME 110.75 Chan 44 (Y)

MISSED APPROACH
Climbing right turn to 4500
direct to WPT03 and hold.

WPT02

WPT01

WPT03

212°

2300

2300

1383

4.0nm   2.3 nm   7.2nm

ELEV 41

8000 X 200

171

22

28

8750 X 150 35

120

169

195

193

241

CATEGORY	A	B	C	D
S-MLS 22	**235-1/2**	200 (200-1/2)		

FOR RESEARCH TESTS ONLY

REIL Rwys 4 and 22
HIRL Rwys 4-22 and 10-28

Knots	60	90	120	150	180
Min:Sec					

MLS RNAV RWY 22 OFFSET

CHINCOTEAGUE ISLAND, VIRGINIA

37° 56'N-75° 28W   CHINCOTEAGUE ISLAND, VIRGINIA
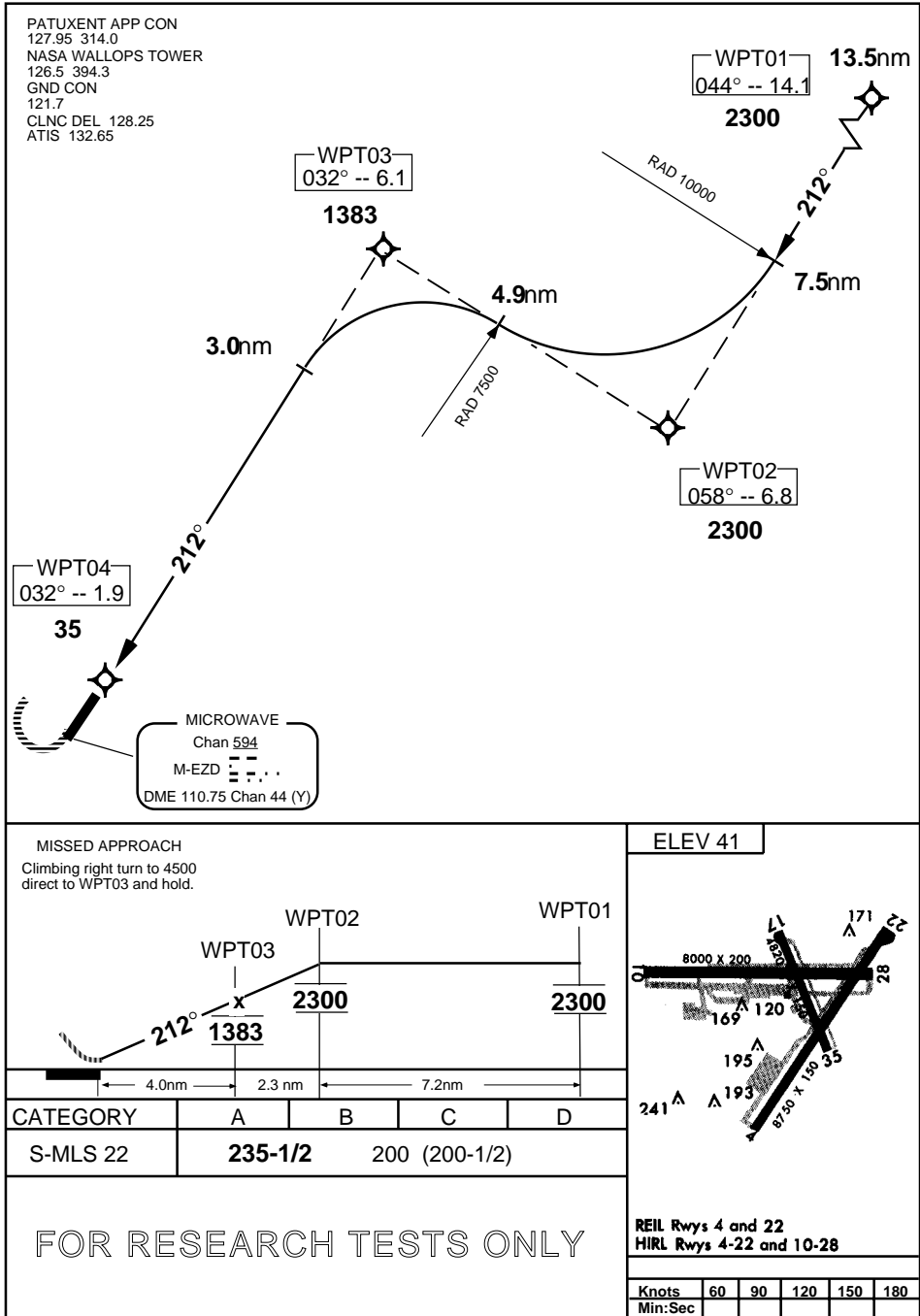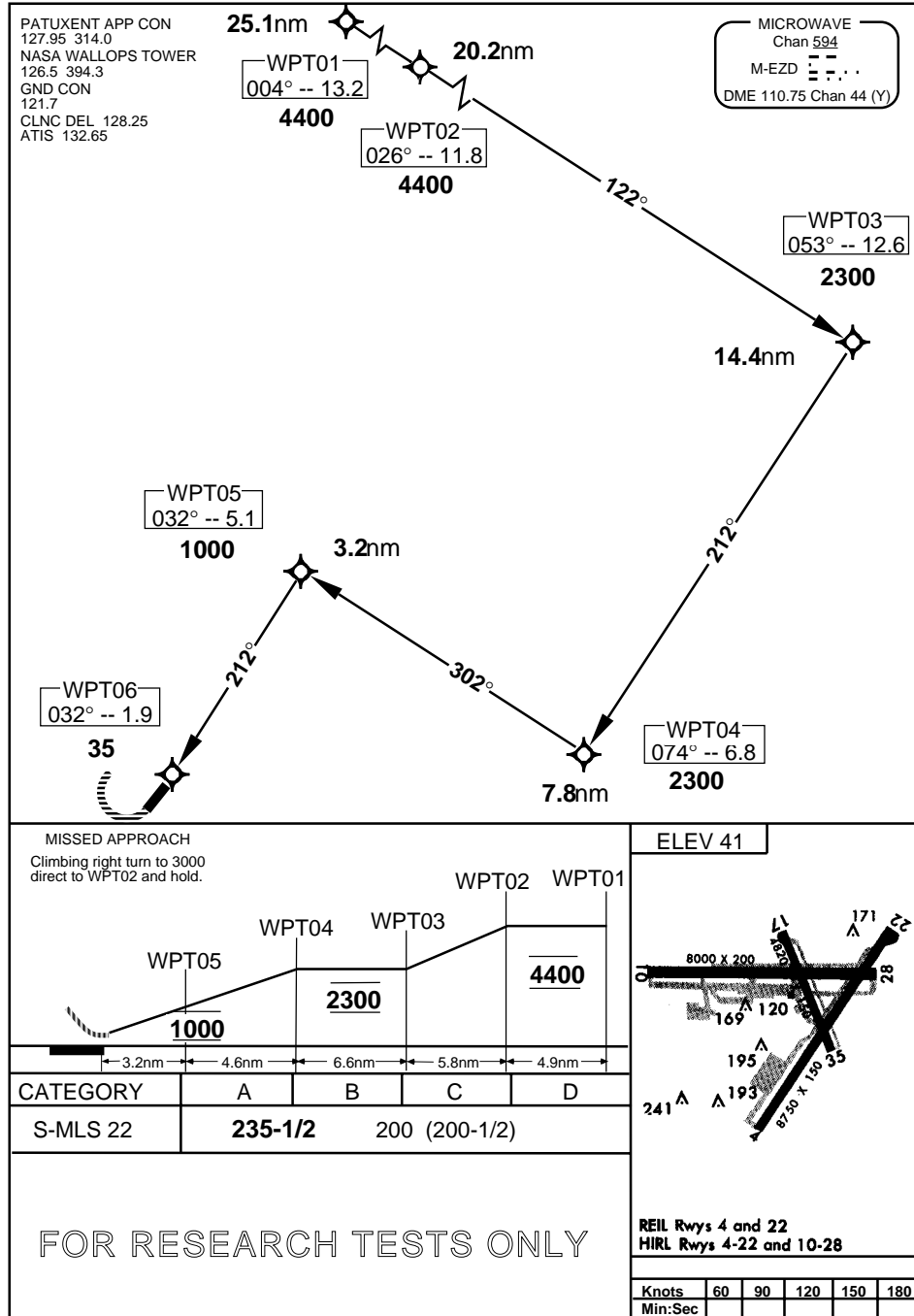CHINCOTEAGUE ISLAND/WALLOPS FLIGHT FACILITY (WAL)

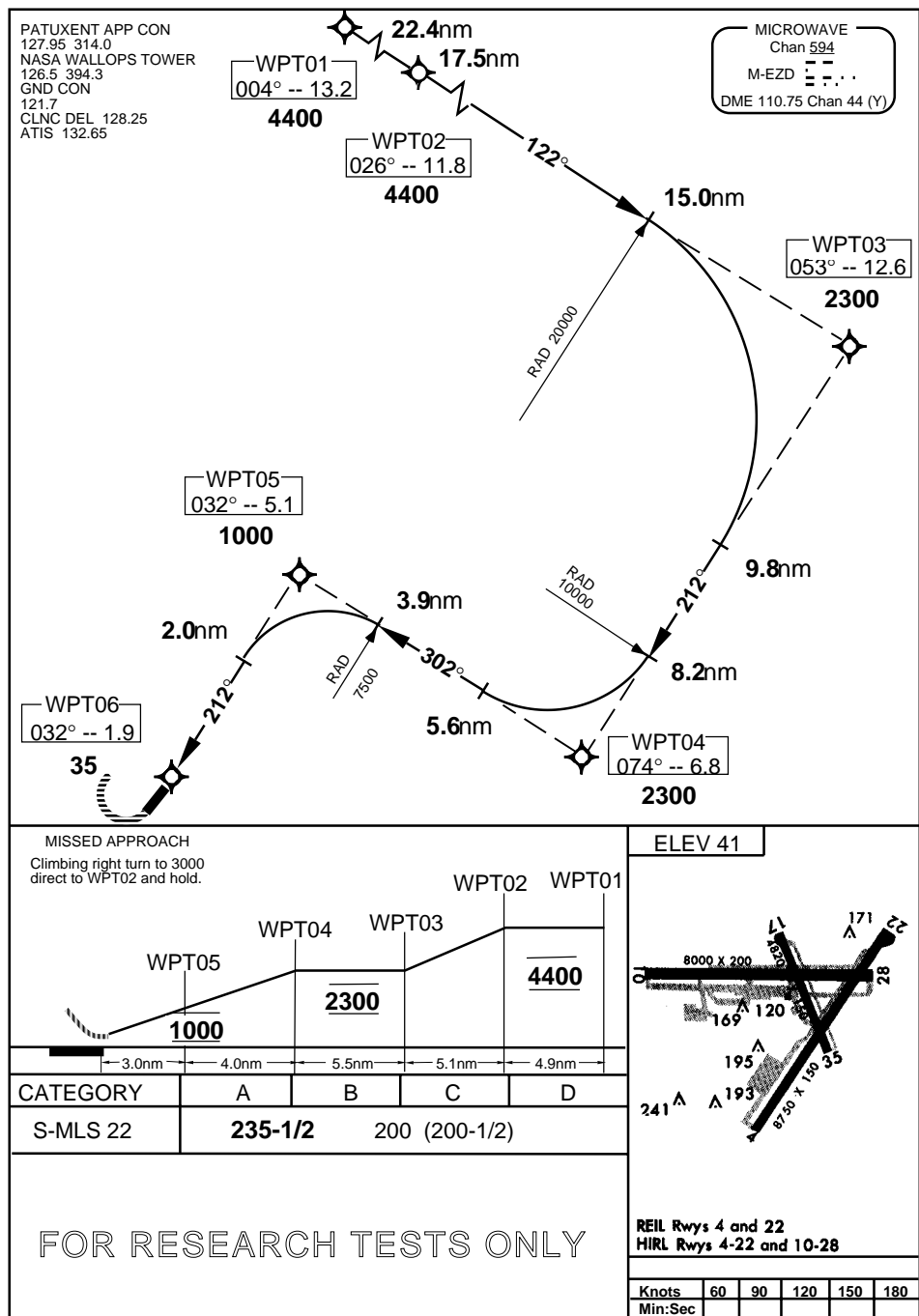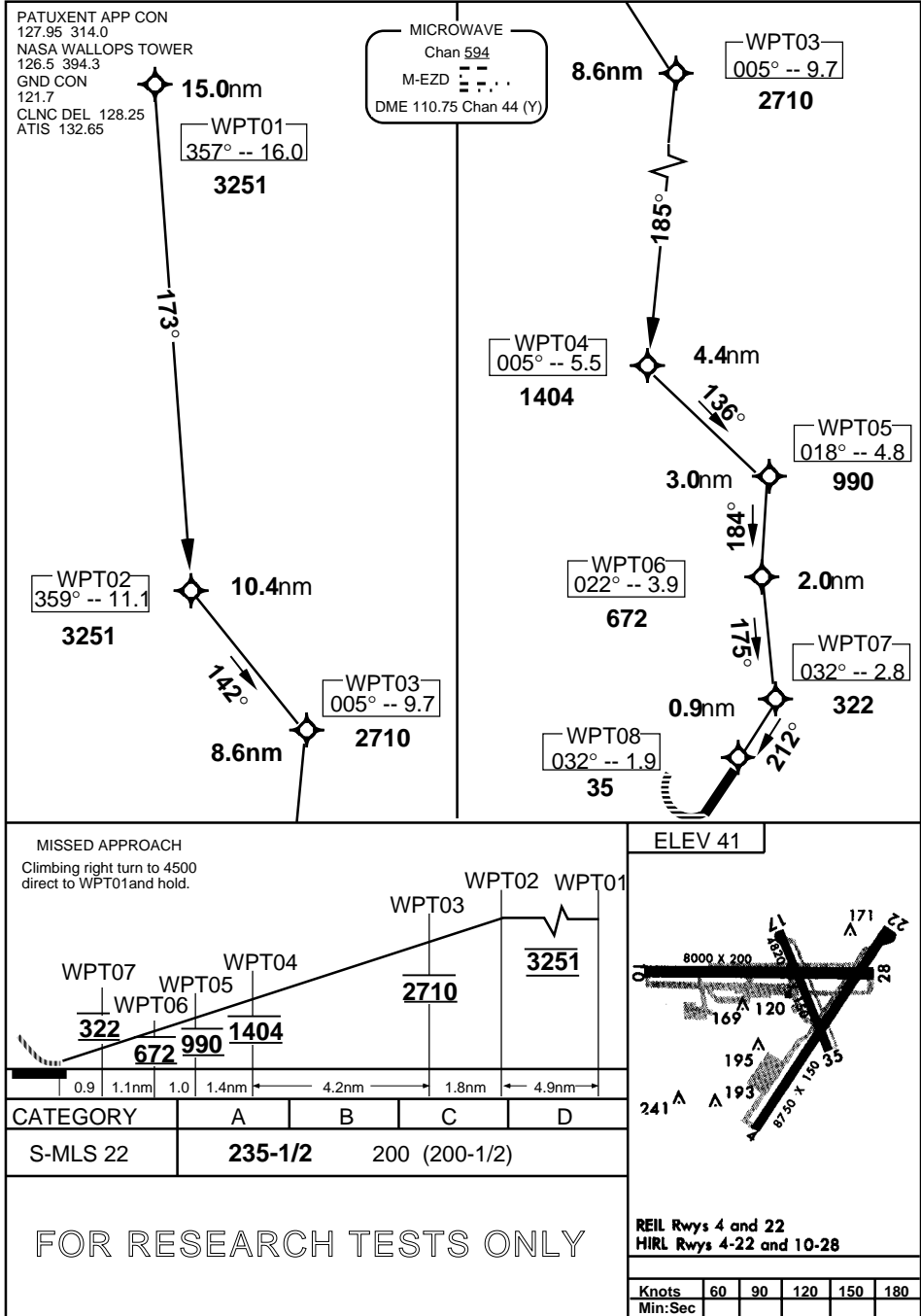Figure 9. OFFSET approach procedure with specified turn radii.

MLS RNAV RWY 22 HOOK

PATUXENT APP CON
127.95 314.0
NASA WALLOPS TOWER
126.5 394.3
GND CON
121.7
CLNC DEL 128.25
ATIS 132.65

MICROWAVE
Chan 594
M-EZD
DME 110.75 Chan 44 (Y)

25.1nm

WPT01
004° -- 13.2
4400

20.2nm

WPT02
026° -- 11.8
4400

122°

WPT03
053° -- 12.6
2300

14.4nm

WPT05
032° -- 5.1
1000

3.2nm

212°

212°

WPT06
032° -- 1.9
35

302°

WPT04
074° -- 6.8
2300

7.8nm

MISSED APPROACH
Climbing right turn to 3000
direct to WPT02 and hold.

ELEV 41

WPT02 WPT01
WPT04 WPT03
WPT05

4400

2300

1000

3.2nm 4.6nm 6.6nm 5.8nm 4.9nm

CATEGORY	A	B	C	D
S-MLS 22	**235-1/2**	200 (200-1/2)		

FOR RESEARCH TESTS ONLY

8000 X 200
171
22
28
169 120
195 35
8750 X 150
241 193

REIL Rwys 4 and 22
HIRL Rwys 4-22 and 10-28

Knots	60	90	120	150	180
Min:Sec					

MLS RNAV RWY 22 HOOK

Figure 10. HOOK approach procedure for segmented algorithm with computed turn radii.

MLS RNAV RWY 22 HOOK

PATUXENT APP CON
127.95 314.0
NASA WALLOPS TOWER
126.5 394.3
GND CON
121.7
CLNC DEL 128.25
ATIS 132.65

MICROWAVE
Chan 594
M-EZD
DME 110.75 Chan 44 (Y)

22.4nm

WPT01
004° -- 13.2
4400

17.5nm

WPT02
026° -- 11.8
4400

122°

15.0nm

WPT03
053° -- 12.6
2300

RAD 20000

WPT05
032° -- 5.1
1000

RAD 10000

212°

9.8nm

3.9nm

2.0nm

212°

RAD 7500

302°

8.2nm

WPT06
032° -- 1.9

35

5.6nm

WPT04
074° -- 6.8
2300

MISSED APPROACH
Climbing right turn to 3000
direct to WPT02 and hold.

ELEV 41

WPT02   WPT01

WPT04   WPT03

WPT05

4400

2300

1000

	3.0nm	4.0nm	5.5nm	5.1nm	4.9nm

CATEGORY	A	B	C	D
S-MLS 22	235-1/2	200 (200-1/2)		

FOR RESEARCH TESTS ONLY

REIL Rwys 4 and 22
HIRL Rwys 4-22 and 10-28

8000 X 200

171
22
28
35
241
195
193
169 120
8750 X 150

Knots	60	90	120	150	180
Min:Sec					

MLS RNAV RWY 22 HOOK
CHINCOTEAGUE ISLAND, VIRGINIA

Figure 11. HOOK approach procedure with specified turn radii.

MLS RNAV RWY 22 RIVER

CHINCOTEAGUE ISLAND/WALLOPS FLIGHT FACILITY (WAL)

CHINCOTEAGUE ISLAND, VIRGINIA

PATUXENT APP CON
127.95 314.0
NASA WALLOPS TOWER
126.5 394.3
GND CON
121.7
CLNC DEL 128.25
ATIS 132.65

MICROWAVE
Chan 594
M-EZD
DME 110.75 Chan 44 (Y)

8.6nm

WPT03
005° -- 9.7
2710

15.0nm

WPT01
357° -- 16.0
3251

185°

173°

WPT04
005° -- 5.5
1404

4.4nm

136°

WPT05
018° -- 4.8
990

3.0nm

184°

WPT02
359° -- 11.1
3251

10.4nm

142°

WPT03
005° -- 9.7
2710

8.6nm

WPT06
022° -- 3.9
672

2.0nm

175°

WPT07
032° -- 2.8
322

0.9nm

212°

WPT08
032° -- 1.9
35

MISSED APPROACH

Climbing right turn to 4500
direct to WPT01 and hold.

ELEV 41

WPT02 WPT01

WPT03

3251

WPT07

WPT04

WPT05

2710

WPT06

322

990 **1404**

672

| | 0.9 | 1.1nm | 1.0 | 1.4nm | 4.2nm | 1.8nm | 4.9nm |

8000 X 200

8750 X 150

REIL Rwys 4 and 22
HIRL Rwys 4-22 and 10-28

CATEGORY	A	B	C	D
S-MLS 22	235-1/2	200 (200-1/2)		

FOR RESEARCH TESTS ONLY

Knots	60	90	120	150	180
Min:Sec					

MLS RNAV RWY 22 RIVER

CHINCOTEAGUE ISLAND, VIRGINIA

CHINCOTEAGUE ISLAND, VIRGINIA

37° 56'N-75° 28W

CHINCOTEAGUE ISLAND/WALLOPS FLIGHT FACILITY (WAL)

Figure 12. RIVER approach for segmented algorithm with computed turn radii.

CHINCOTEAGUE ISLAND/WALLOPS FLIGHT FACILITY (WAL)

MLS RNAV RWY 22 RIVER
CHINCOTEAGUE ISLAND, VIRGINIA

PATUXENT APP CON
127.95 314.0
NASA WALLOPS TOWER
126.5 394.3
GND CON
121.7
CLNC DEL 128.25
ATIS 132.65

MICROWAVE
Chan 594
M-EZD
DME 110.75 Chan 44 (Y)

15.0nm

WPT01
357° -- 16.0
3251

WPT03
005° -- 9.7
2710

185°

5.0nm

173°

WPT04
005° -- 5.5
1404

3.6nm

RAD 12500

136°

WPT05
018° -- 4.8
990

10.7nm

WPT02
359° -- 11.1
3251

WPT06
022° -- 3.9
672

184°

2.1nm

142°

9.2nm

175°

1.3nm

RAD 10000

0.5nm

WPT07
032° -- 2.8
322

WPT03
005° -- 9.7
2710

WPT08
032° -- 1.9
35

212°

MISSED APPROACH

Climbing right turn to 4500
direct to WPT01and hold.

ELEV 41

WPT02   WPT01

WPT03

3251

WPT07   WPT04

2710

WPT05

WPT06

322

1404

672   990

8000 X 200

171

120

169

195

193

241

8750 X 150

| | 1.0 | 1.1nm | 1.0 | 1.3nm | 4.1nm | 1.7nm | 4.9nm |

CATEGORY	A	B	C	D
S-MLS 22	235-1/2	200 (200-1/2)		

NOTE: ALL TURN RADII 7500' UNLESS OTHERWISE SHOWN.

FOR RESEARCH TESTS ONLY
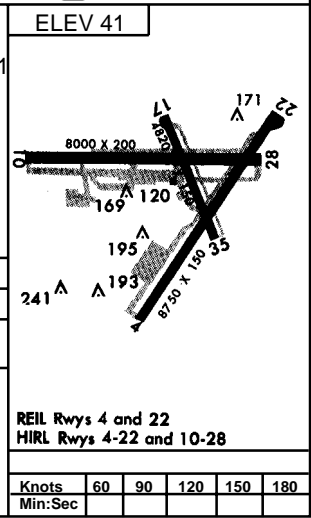
REIL Rwys 4 and 22
HIRL Rwys 4-22 and 10-28

Knots	60	90	120	150	180
Min:Sec					

MLS RNAV RWY 22 RIVER
CHINCOTEAGUE ISLAND, VIRGINIA

37° 56'N-75° 28W   CHINCOTEAGUE ISLAND, VIRGINIA
CHINCOTEAGUE ISLAND/WALLOPS FLIGHT FACILITY (WAL)

Figure 13. RIVER approach procedure with specified turn radii.
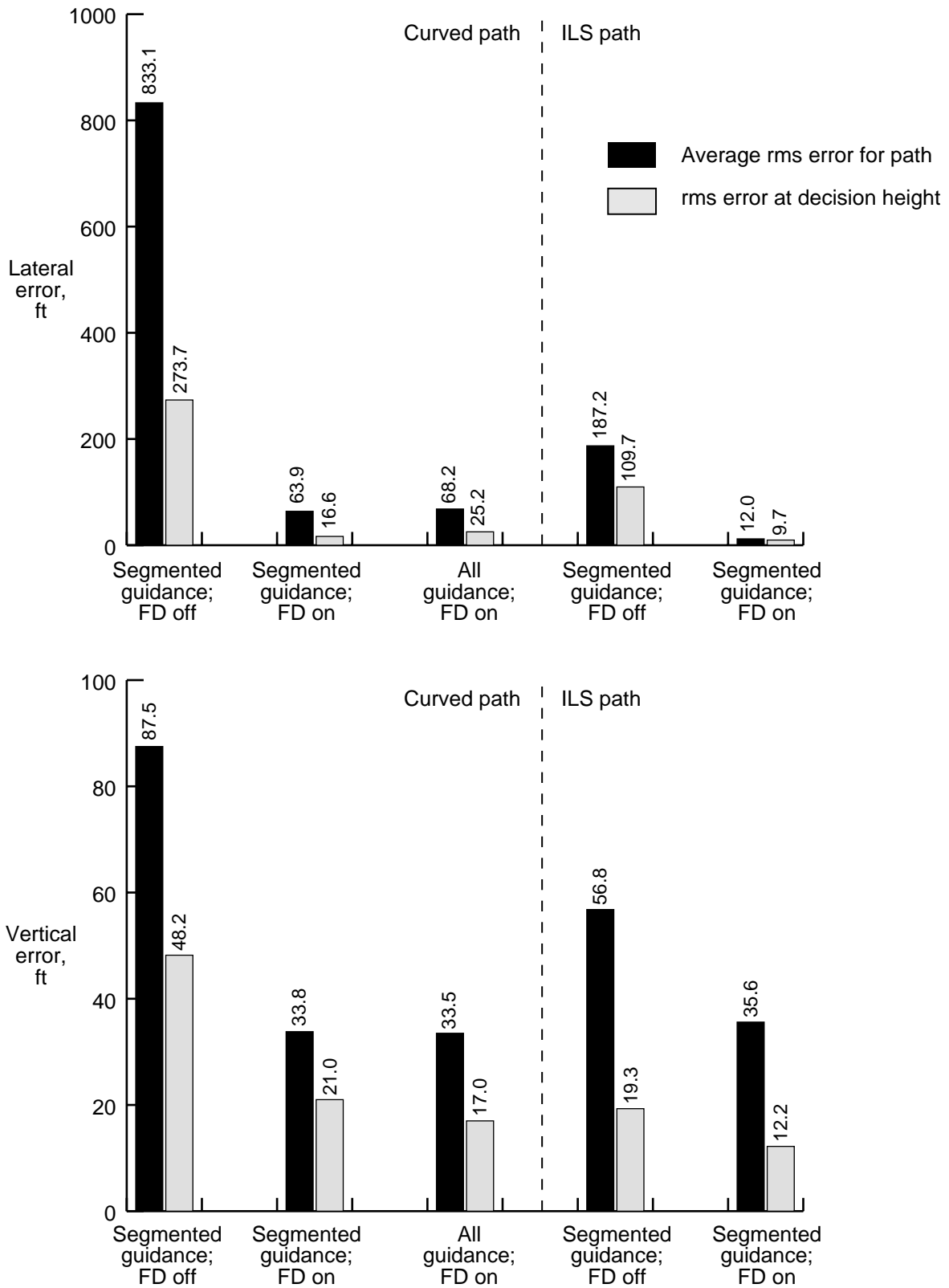
Figure 14. rms path tracking errors for approaches with and without flight director commands.

Figure 15. Control column and wheel activity for the approaches with and without flight director commands.

Figure 16. rms path tracking errors for each situation information algorithm with flight director commands.
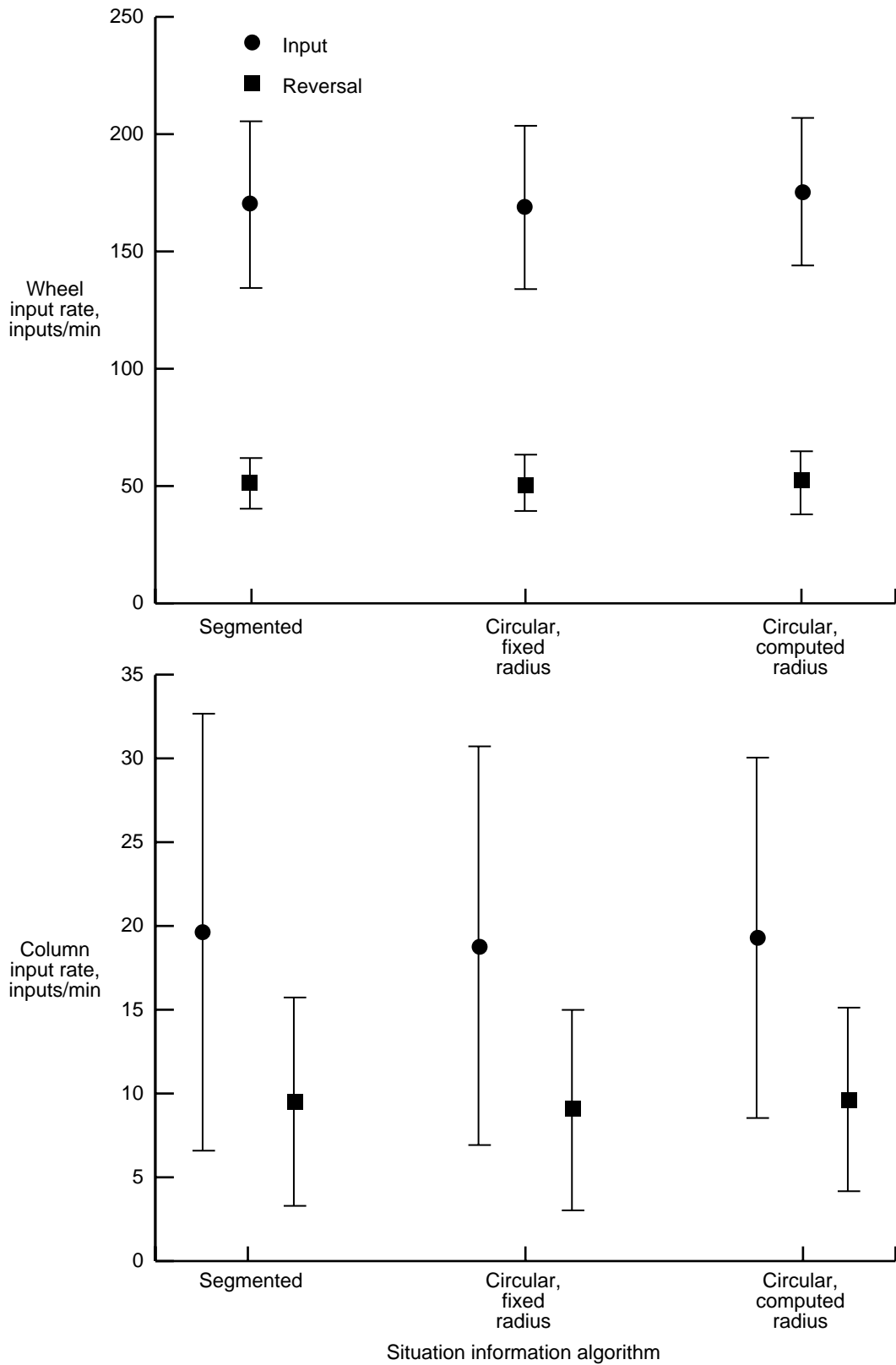
Figure 17. Control column and wheel activity for each situation information algorithm with flight director commands.
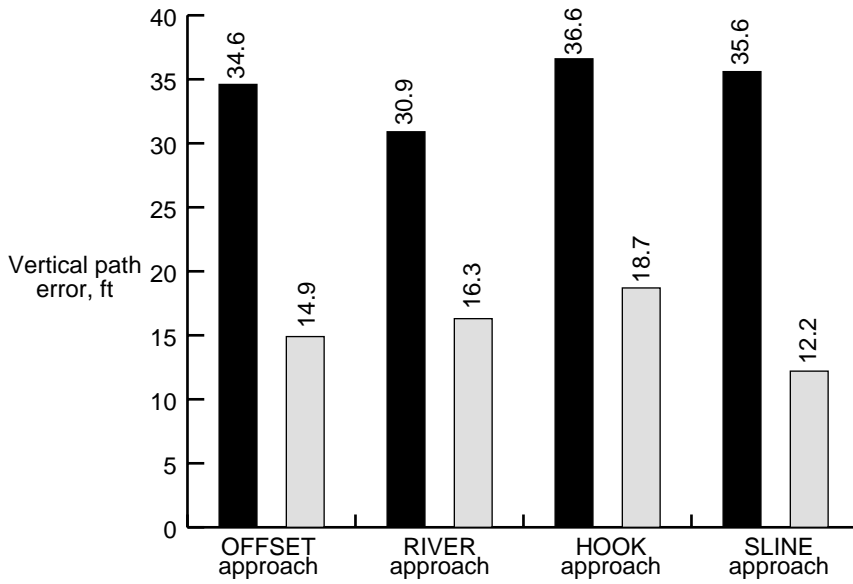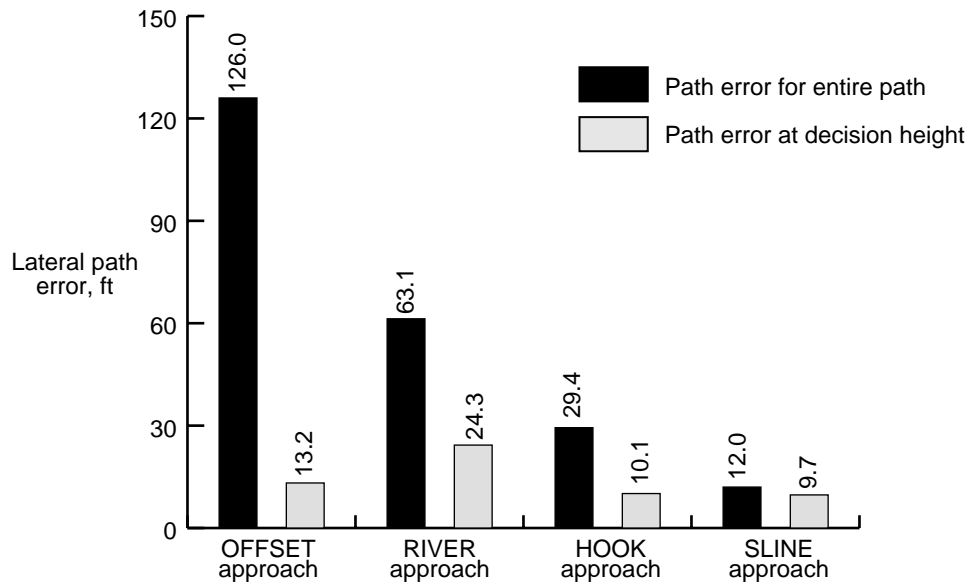
Figure 18. rms path tracking errors for each approach with flight director commands.

Figure 19. Control column and wheel activity for each approach with flight director commands.

L-85-9008

Figure 1. Flight instrument arrangement.

L-85-6843

Figure 2. Attitude director indicator instrument.

L-85-6846

Figure 3. Horizontal situation indicator instrument.

Figure 8. OFFSET approach procedure for segmented algorithm with computed turn radii.

Figure 9. OFFSET approach procedure with specified turn radii.

Figure 10. HOOK approach procedure for segmented algorithm with computed turn radii.

Figure 11. HOOK approach procedure with specified turn radii.

Figure 12. RIVER approach for segmented algorithm with computed turn radii.

Figure 13. RIVER approach procedure with specified turn radii.

Figure 14. rms path tracking errors for approaches with and without flight director commands.

Figure 15. Control column and wheel activity for the approaches with and without flight director commands.

Figure 16. rms path tracking errors for each situation information algorithm with flight director commands.

Figure 17. Control column and wheel activity for each situation information algorithm with flight director commands.

Figure 18. rms path tracking errors for each approach with flight director commands.

Figure 19. Control column and wheel activity for each approach with flight director commands.

1. AGENCY USE ONLY *(Leave blank)*	2. REPORT DATE February 1993	3. REPORT TYPE AND DATES COVERED Technical Paper

4. TITLE AND SUBTITLE

Manual Flying of Curved Precision Approaches to Landing With Electromechanical Instrumentation
A Piloted Simulation Study

5. FUNDING NUMBERS

WU 505-64-13-01

6. AUTHOR(S)

Charles E. Knox

7. PERFORMING ORGANIZATION NAME(S) AND ADDRESS(ES)

NASA Langley Research Center
Hampton, VA 23681-0001

8. PERFORMING ORGANIZATION REPORT NUMBER

L-16964

9. SPONSORING/MONITORING AGENCY NAME(S) AND ADDRESS(ES)

National Aeronautics and Space Administration
Washington, DC 20546-0001

10. SPONSORING/MONITORING AGENCY REPORT NUMBER

NASA TP-3255

11. SUPPLEMENTARY NOTES

12a. DISTRIBUTION/AVAILABILITY STATEMENT

Unclassified–Unlimited

Subject Category 06

12b. DISTRIBUTION CODE

13. ABSTRACT *(Maximum 200 words)*

A piloted simulation study was conducted to examine the requirements for using electromechanical flight instrumentation to provide situation information and flight guidance for manually controlled flight along curved precision approach paths to a landing. Six pilots were used as test subjects. The data from these tests indicated that flight director guidance is required for the manually controlled flight of a jet transport airplane on curved approach paths. Acceptable path tracking performance was attained with each of the three situation information algorithms tested. Approach paths with both multiple sequential turns and short final path segments were evaluated. Pilot comments indicated that all the approach paths tested could be used in normal airline operations.

14. SUBJECT TERMS

MLS; Airplane; Guidance; Approach procedures; Flight instrumentation

15. NUMBER OF PAGES

39

16. PRICE CODE

A03

17. SECURITY CLASSIFICATION OF REPORT Unclassified	18. SECURITY CLASSIFICATION OF THIS PAGE Unclassified	19. SECURITY CLASSIFICATION OF ABSTRACT	20. LIMITATION OF ABSTRACT